Quinoxaline-annelated Z-shaped quadruple-bridged orthocyclophanes: synthesis and crystal structures

Teh-Chang Chou [a,b,*], Kung-Ching Liao [b]

[a] Department of Applied Chemistry, Chaoyang University of Technology, Wufong, Taichung 41369, Taiwan
[b] Department of Chemistry and Biochemistry, National Chung Cheng University, Minsyong, Chiayi 621, Taiwan

ABSTRACT

A three-step synthesis of nineteen Z-shaped quadruple-bridged [6,6] and [6,4]orthocyclophanes comprising two quinoxaline-based sidewalls are described. The synthesis began from the bis-Diels–Alder adducts **B1**–**B3** followed by ruthenium-promoted oxidation of dichloroetheno-bridges in the adducts to generate a bis-α-diketones, which were then condensed with various arene-1,2-diamines (**9a**–**g**) to construct sidewalls (phane parts) of Z-shaped quadruple-bridged orthocyclophanes **D1-3**, **D2g**, and **D3g**. Single-crystal structures of six orthocyclophanes (**D1a**, **D2a**, **D2f**, **D3f**, **D2g-α**, and **D3g-α**) were obtained and revealed that the C_{Ar}—H···π and π···π stacking interactions between N-containing arene rings are the major driving force for molecular assembly and crystal packing, in addition to the interactions involving the polar OCH_3 groups and the solvate molecules.

© 2010 Elsevier Ltd. All rights reserved.

1. Introduction

Noncovalent intermolecular interactions, such as ion-pairing, hydrogen bonding, and arene–arene interactions, play a central role in manipulating the processes of molecular recognition and self-assembly to form highly organized structure systems (supermolecules) of biological and practical importance.[1] The attractive nonbonded interactions involving aromatic rings (arene–arene interactions) comprise π–π stacking, X—H/π, and cation/π interactions as the major forces[2] that are frequently found in stabilizing the base pair stacking in DNA, protein folding, host–guest binding, drug receptor interactions, and crystal engineering.[3–5] Various prospective applications have been disclosed and inspired growing intenseness of synthetic endeavor directed toward the search for the new arene π-systems of specially designed architecture that may possess specific functions for such applications.[6] In this context, rigid and often symmetric polycarbocyclic skeletons are frequently utilized to serve as 'platforms' for the attachment of functional groups or ligands, which demonstrate the role of arene–arene interactions in long-range electron/energy transfer phenomena,[7] self-assembly,[8] and the formation of the host–guest complexes.[9]

Recently, we developed an efficient synthetic process for the construction of quinoxaline-based U-shaped multi-bridged [n,n′] orthocyclophanes having generic structure **A**.[10] This process consists of three fundamental operations: (1) using 1,2,3,4-tetrachloro-5,5-dimethoxycyclopentadiene (TDCp, **1**)[11] to react with a bis-dienophile, such as cyclohexa-1,4-diene (**2**), cycloocta-1,5-diene (**3**), or N-substituted dioxa-bridged hexahydronaphthalene **4**, for the preparation of a Diels–Alder bis-adduct serving as the central scaffold, (2) transforming the dichloroetheno-bridges in the bis-adduct to generate a bis-α-diketone by ruthenium-promoted oxidation,[12] followed by (3) constructing sidewalls by the condensation of bis-α-diketone with an arene-1,2-diamine (ADA) to produce [n,n′]orthocyclophanes embedded with quinoxaline-based aromatic rings. The versatility of the process is manifested by the presence of two changeable substructures, the intercalator and the quinoxaline ring. The intercalator originated from the bis-dienophilic cycloalkadiene can serve as the controller of the size and shape of polycyclic scaffold, and consequently the distance and stereo-alignment between two quinoxaline rings, the motif of which is derived from various ADA's. The U- or the Z-shape of [n,n′]orthocyclophanes, that is, the syn or anti stereo-alignment of two quinoxaline rings, is predestined by the π-facial selectivity of Diels–Alder reaction between **1** and cyclic bis-dienophile, which in most cases is well-established and predictable. The presence of amendable functional groups in the intercalator would amplify the usefulness of this process. The results of

* Corresponding author. Tel.: +886 4 2332 3000x4309; fax: +886 4 2374 2341; e-mail address: tcchou@cyut.edu.tw (T.-C. Chou).
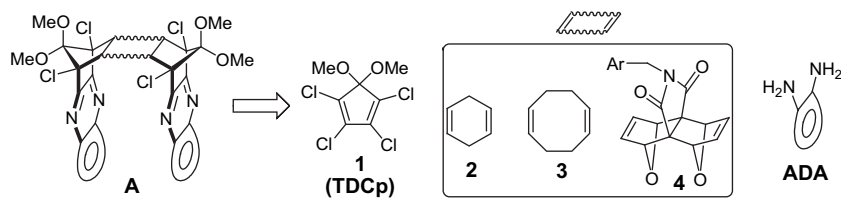
synthesizing the U-shaped multi-bridged [n,n′]orthocyclophanes **A**[10] suggested that the synthetic process appeared to be practical and prompted us to further exploit the practicability of synthetic process outlined in Scheme 1 for the synthesis of Z-shaped quadruple-bridged [n,n′]orthocyclophanes **D**, utilizing known Diels–Alder bis-adducts **B1**–**B3**. Among them, the benzoquinoxaline-walled orthocyclophane **D1f** was previously synthesized as a reference compound for studying luminescence properties of U-shaped quinoxaline-based orthocyclophanes.[10a] The newly synthesized Z-shaped [n,n′]orthocyclophanes **D** showed luminescence properties similar to **D1f** (see Experimental section) and did not disclose different results, when compared with the corresponding U-shaped [n,n′]orthocyclophanes. In this paper we primarily describe the synthetic implementation and solid-state structures of some Z-shaped [n,n′]orthocyclophanes, which show arene–arene interactions as the major forces in the crystal packing.

## 2. Results and discussion

2.1. Synthesis

All the bis-adducts **B1**–**B3** were known and readily accessible as shown in Scheme 2. The *endo,anti,endo* bis-cycloadduct **B1**, along with the easily separable *endo,syn,endo* bis-cycloadduct **B1′**, was obtained from the Diels–Alder reaction of cycloocta-1,5-diene (**3**) with TDCp (**1**).[13] Bis-adduct **B3** could be attained straightforwardly from the Diels–Alder reaction of TDCp with naphthalene (**8**), albeit under harsh condition (neat, 165 °C, 12 days) and in low yield (45%).[14] However, bis-adduct **B2**,[15] a formal bis-adduct of TDCp and benzene, could only be realized indirectly via the Diels–Alder reaction of TDCp with tricyclic 1,3-cyclohexadiene **7**, which was prepared form the Diels–Alder adduct **6** of *p*-benzoquinone (**5**) and TDCp as shown in Scheme 2.[16] Both bis-adducts **B2** and **B3** are
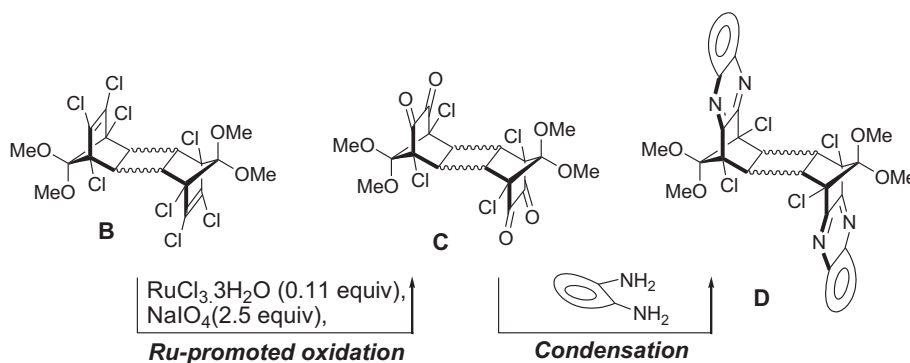
**Scheme 1.** Synthetic strategy for the construction of Z-shaped quinoxaline-based orthocyclophanes **D**'s.
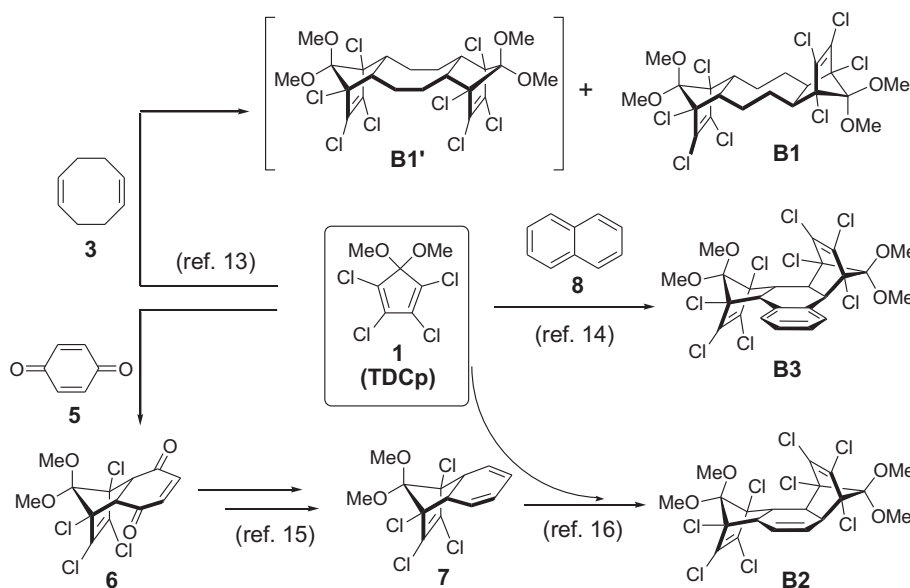
Scheme 2. Preparation of the Diels–Alder bis-adducts **B**'s.
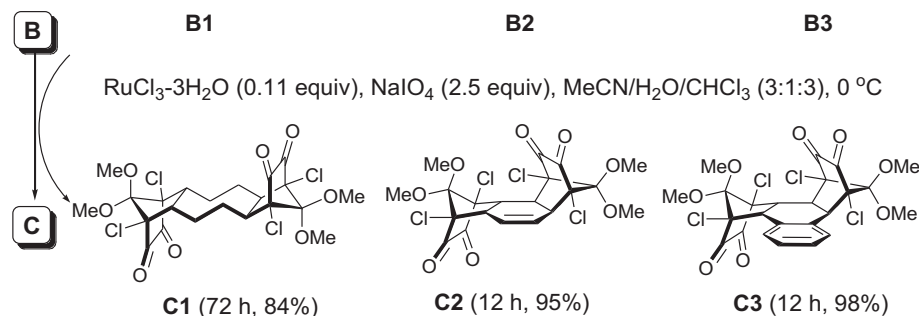
Scheme 3. Synthesis of Z-shaped bis-α-diketones **C**'s.

chiral and thus were produced as a racemic mixture composed of equal amount of *P*- and *M*-forms. The conversion of bis-adducts **B's** to the corresponding bis-α-diketones **C's** essentially followed the ruthenium-promoted oxidation procedure reported by Khan et al.,[12] and the results are summarized in Scheme 3. Thus, when employing RuCl$_3$·3H$_2$O as promoter (0.11 equiv), NaIO$_4$ as oxidant (2.5 equiv), and stirring at 0 °C in the solvent system of CHCl$_3$/MeCN/H$_2$O (3:3:1) for a period of time, the reactions smoothly provided yellow bis-α-diketones **C1**–**C3** in good yields. The infrared spectra showed two strong carbonyl absorption bands at 1760–1800 cm^{-1}, appropriate to strained cyclic bis-α-diketones. Due to the poor solubility of **C1** in common NMR solvents, only the ^{13}C NMR spectra of **C2** and **C3** were obtained, each of which contained two signals at δ 185–189 and supported the presence of α-dicarbonyl group.

The condensation reactions of bis-α-diketones **C's** with arene-1,2-diamines to achieve the synthesis of Z-shaped quinoxaline-based orthocyclophanes **D's** were next carried out. As shown in Scheme 4, the condensation reactions were executed by performing the reactions of bis-α-diketones **C's** with 2.20 equiv of ADA's (**9**) in PhCl (0.04 M) at refluxing temperature and in the presence of 0.10 equiv of Zn(OAc)$_2$ as a catalyst. Utilizing this condensation reaction procedure, we successfully obtained quadruple-bridged [6,6] orthocyclophanes **D1**'s and racemic [6,4]orthocyclophanes **D2**'s and **D3**'s in yields of more than 90% from the reactions of corresponding bis-α-diketones **C's** with various 4,5-disubstituted ADA's, **9a**–**f**. As indicated in Scheme 4, bis-α-diketones **C2/C3** took much less time to complete the reactions with ADA's than bis-α-diketone **C1**. This fact implies that the nucleophilic addition of ADA's to the carbonyl groups occurs on the concave side (anti to the dimethoxymethano
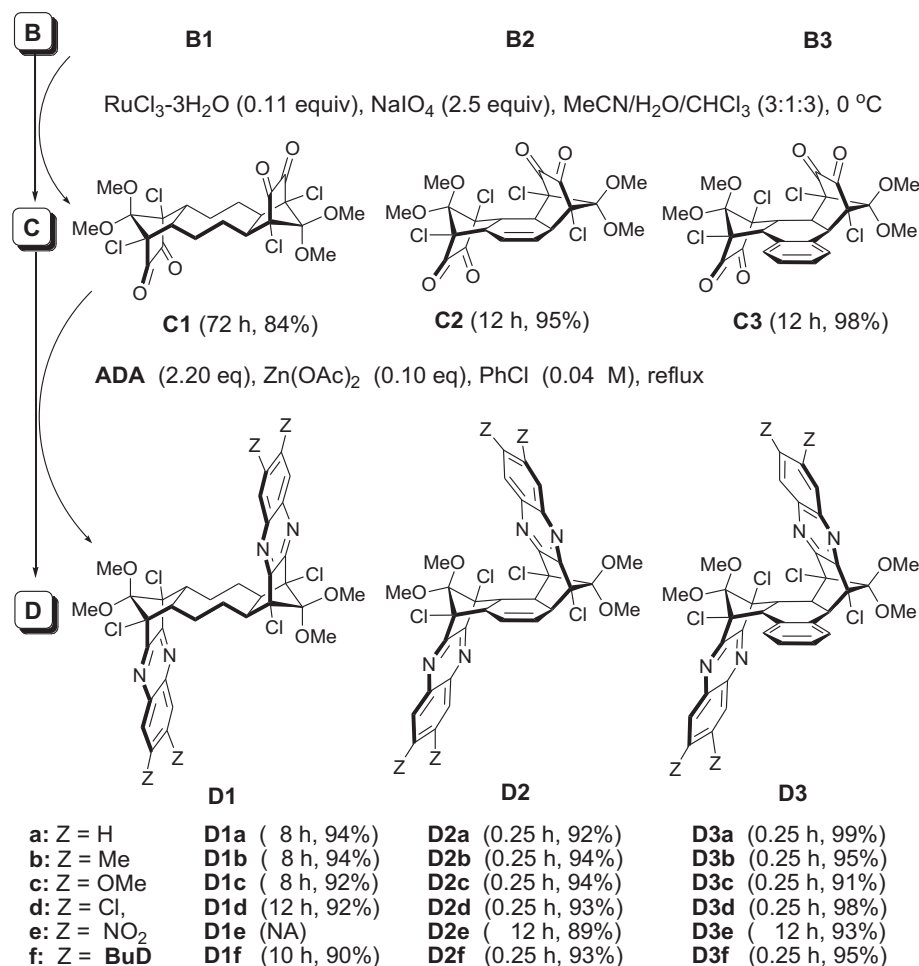
Scheme 4. Synthesis of Z-shaped quinoxaline-based orthocyclophanes **D**'s.

bridge) of bis-α-diketones, in which the saturated intercalator of **C1** is more steric demanding due to inward hydrogen atoms. The use of PhCl as solvent is essential in ensuring a good yield, and in most cases, the reactions were clean, requiring only filtration and re-crystallization in handling the reaction product mixtures.

The Z-shaped orthocyclophanes synthesized (Scheme 4) exhibit conformational rigidity and symmetry-reflected ^{1}H and ^{13}C NMR spectra. The quadruple-bridged [6,6]orthocyclophanes **D1a–f** display NMR spectra reflecting the expected inherent C_{2v}-symmetry. For example, benzoquinoxaline derivative **D1f** having molecular formula $C_{42}H_{36}Cl_4N_4O_4$ shows a twelve-line ^{13}C NMR spectrum and a ^{1}H NMR spectrum containing 10 groups of absorptions. In particular, a distinct four-proton absorption signal appears at much higher magnetic field than the other C(sp^3)–H in the ^{1}H NMR spectra of **D1a–f** (e.g., **D1a**: δ 0.07 vs δ 2.71/2.10 and **D1f**: δ 0.19 vs δ 2.72/2.15). This signal is ascribed to the methylene protons lying parallel to (on top of) and most closely to the heteroaromatic ring, as a result of anisotropic shielding effect,[17] a situation similar to the precursor **B1** (δ 2.67/2.10/0.80) where anisotropic shielding effect of C=C is operating. On the other hand, the inherent C_2-symmetry expected for quadruple-bridged [6,4]orthocyclophanes **D2**'s and **D3**'s is evidently demonstrated by a ^{13}C NMR spectrum containing the number of absorption line equal to half of the total number of constituent carbon atoms, and a ^{1}H NMR spectrum showing matching groups of absorptions (see Experimental section). It was also noticed that, due to anisotropic shielding effect, the absorption signals for vinyl protons in **D2**'s (δ 5.17–5.25) and phenyl protons in **D3**'s (δ 6.80–7.00/6.79–7.00) shifted upfield comparing, respectively, with the corresponding protons in **B2** (δ 5.82) and **B3** (δ 7.07/7.53).

We furthermore subjected an unsymmetrical ADA, pyridine-2,3-diamine (**9g**), to the condensation reaction with bis-α-diketones **C2** and **C3**. Due to decomposition of **9g** in refluxing chlorobenzene, which was used as solvent in the preparation of **D1-3** (Scheme 4), toluene was used instead for the synthesis of **D2g** and **D3g** (Scheme 5). In principle, the reaction could yield three stereoisomeric products, **D2g-α** (**D3g-α**), **D2g-β** (**D3g-β**), and **D2g-γ** (**D3g-γ**), differentiated by the orientation of two nitrogen atoms of pyridine rings relative to the C=C (benzene ring), as shown in Scheme 5. Compounds **D2g-α** (**D3g-α**) and **D2g-β** (**D3g-β**), in which the nitrogen atoms of pyridine rings are situated, respectively, at opposite and same side to the C=C (benzene ring) moiety, are C_2-symmetric. Compounds **D2g-γ** and **D3g-γ** have no symmetry

element and are C_s-symmetric. In practice, we isolated a major product from the reaction of bis-α-diketone **C2** and diamine **9g** in 81% yield, which displayed a fifteen-line ^{13}C NMR spectrum and a ^{1}H NMR spectrum containing eight groups of absorptions for a molecular formula of $C_{30}H_{24}Cl_4N_6O_4$. The NMR spectral data could immediately eliminate **D2g-γ** to be the product, but could not discriminate between C_2-symmetric **D2g-α** and **D2g-β**. Similar outcome was observed for the reaction of bis-α-diketone **C3** and diamine **9g**, from which **D3g-α** or **D3g-β** was obtained in 76% yield. The structural determination for the major product in two cases was secured by recourse of X-ray crystallographic analysis and proved to be **D2g-α** and **D3g-α** (vide infra).[18]

2.2. Crystallographic study

2.2.1. Molecular structures. Among the synthesized orthocyclophanes shown in Schemes 4 and 5, we obtained single crystals of **D1a**, **D2a**, **D2f**, **D3f**, **D2g-α**, and **D3g-α** that were suitable for room-temperature X-ray crystal structure determination by re-crystallization from solvent system of EtOH and CH_2Cl_2 or $CHCl_3$.[18] Fig. 1 depicts the molecular structures of **D1a**, **D2a**, **D2f**, **D3f**, **D2g-α**, and **D3g-α** in the crystal. Their crystal data/structure refinement are compiled in Table 3. All orthocyclophanes assume Z-shaped geometry, predestined by the stereochemistry of Diels–Alder bis-adducts **B1-3**, where the phane sidewalls (quinoxaline rings) are pointed away from each other in antiparallel manner (**D1**) or helix mode (**D2**'s and **D3**'s). Due to the rigidity of the norbornenyl rings, the eight-membered ring in **D1a** is induced to fuse at the junction sites with near-zero torsion angles (5.3° and 1.7°) and adopts nearly ideal chair conformation (+116.8°)[19] as indicated by the torsion angles of 122.6° and 115.6° about the C–C bonds that comprise the arms of the chair and connect norbornenyl rings. On the other hand, the rigidity of the norbornenyl rings force cyclohexene ring (intercalator) of **D2a**, **D2f**, and **D2g-α** to adopt a conformation with great deviations from ideal half-chair form of cyclohexene.[20] The double bond is distorted and deviated from planarity with C–C=C–C torsion angle of 7.6°, 8.9°, and 7.6° for **D2a**, **D2f**, and **D2g-α**, respectively. Likewise, the conformation of benzene-fused cyclohexene ring in **D3f** and **D3g-α** is greatly deviated from ideal half-chair form. The bridged C=C bond of benzocyclohexene ring is even more distorted and greatly deviated from planarity with C–C=C–C torsion angle of 24.8° and 21.4° for **D3f** and **D3g-α**,
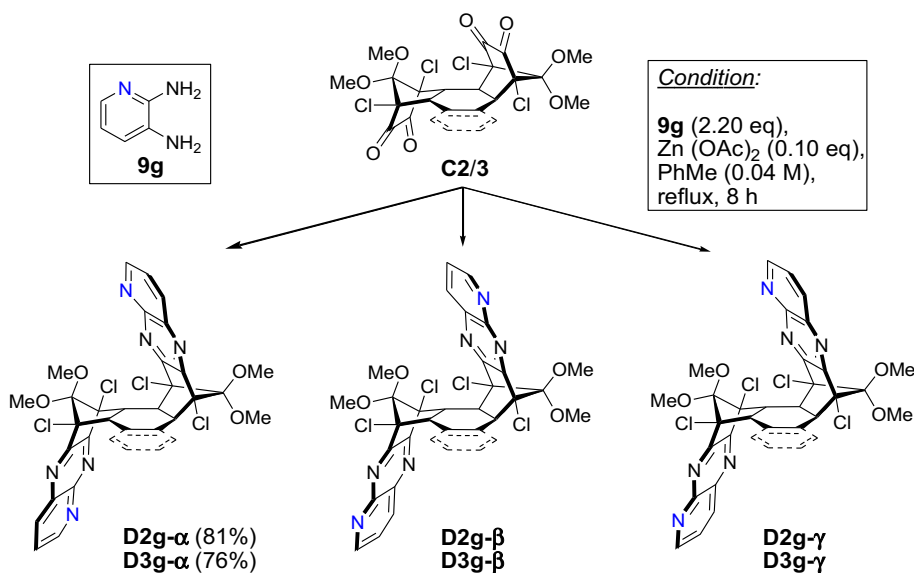
Scheme 5. Reactions of bis-α-diketones **C2/C3** with pyridine-2,3-diamine.
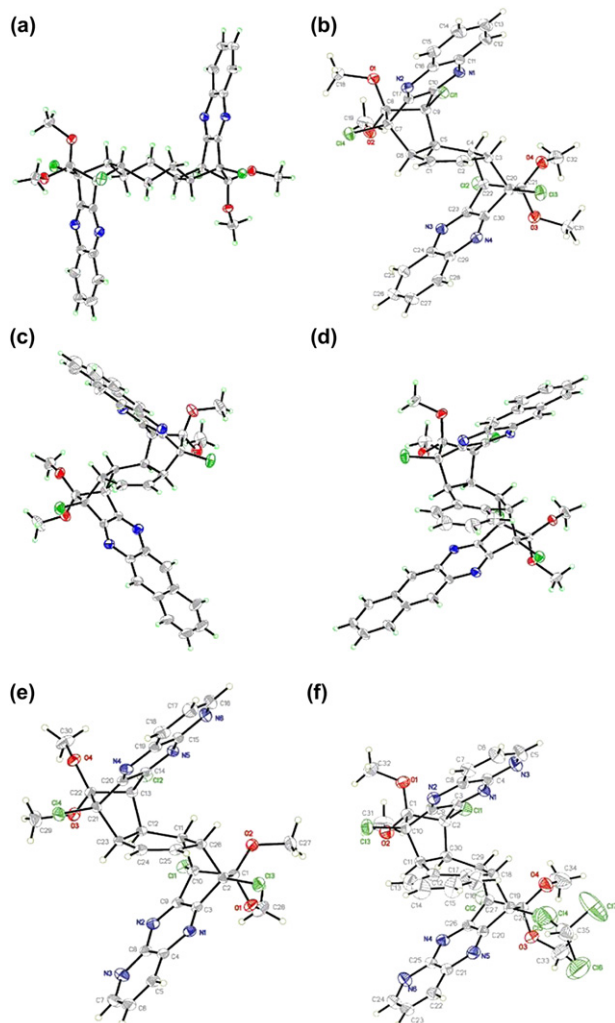
Fig. 1. ORTEP drawings of the crystal structures. The thermal ellipsoids are drawn at the 30% level of probability. (a) **D1a**, (b) **D2a**, (c) **D2f**, (d) **D3f**, (e) **D2g-α**, (f) **D3g-α**, containing a molecule of solvating $CHCl_3$. Color coding: C, gray; H, green; N, blue; O, red, Cl, green.

resulting in twisting benzene subunit at fused junction by 8.8° and 7.1°, respectively.

2.2.2. Crystal packing. In the previous study on the crystal packing of the U-shaped septuple-bridged [7,7]orthocyclophanes (generic formula **A**),[10b] we disclosed that noncovalent interactions relating the quinoxaline rings with their embedded nitrogen atoms, the polar methoxy groups at bridging carbons, and the solvating molecules, are the key driving forces for assembling molecules of this class to form three-dimensional crystalline architectures in the crystals. In this section, we describe similar noncovalent interactions observed in controlling the packing of the Z-shaped orthocyclophanes **D**'s into two- and three-dimensional structures in the crystal. Table 1 lists some selected parameters from the X-ray crystal structures, which describe the structure and packing motifs involving aryl and methoxy groups. Some selected packing motifs in the crystal structures of **D1a**, **D2f**, **D3f**, and **D3g-α** having the participation of solvating molecules are outlined in Table 2.

The quadruple-bridged [6,6]orthocyclophane **D1a** crystallizes from CH_2Cl_2/EtOH solution in the monoclinic space group $P2(1)/c$. An examination of the crystal packing of **D1a** reveals that every molecule of **D1a** carries a solvating CH_2Cl_2 molecule on one of its two quinoxaline rings by N···H−C hydrogen bond [$d_{N···H}$ ($\angle$)=

2.49 Å (140.9°)] and Ar−H···Cl close contact [$d_{Cl···H}$ ($\angle$)=3.15 Å (108.5°), Table 2].[21,22] As shown in Fig. 2 and Table 1, molecules of **D1a** employ their solvated quinoxaline ring to connect the nearby, perpendicularly aligned molecule of **D1a** chiefly by $C_{Ar}H···\pi$ and $OCH_3···\pi$ interactions, forming a two-dimensional molecular sheet on *ab*-plane. The $C_{Ar}H···\pi$ interaction[2f,g] is endowed with N···H hydrogen bond [$d_{N···H}$ ($\angle$)=2.73 Å (155.0°)] and short C···H distances (3.12/3.17 Å) between two quinoxaline rings, which adopt edge-to-face herringbone (face-tilted-T) structure[2a,23] with dihedral angle of about 70° and a centroid-to-centroid distance of 6.57 Å. This two-dimensional molecular array of **D1a** is reinforced by additional interactions between their polarized methoxy groups via OC−H···O hydrogen bonds [$d_{O···H}$ ($\angle$)=2.74 (148.7°) and 2.78 (157.8°)],[1c,24] and by using the solvated quinoxaline ring to attain bilateral $OCH_3···\pi$ interactions with the polarized C−H bonds of OCH_3 group in the neighboring molecules of **D1a**. As indicated in Fig. 2, the $OCH_3···\pi$ interaction on one side is denoted by the OC−H···N_{Ar} hydrogen bond [$d_{N···H}$ ($\angle$)=2.80 Å (131.0°)] and short C−H···C_{Ar} distances (2.83−4.51 Å, π-centroid···H−C distance 3.07 Å), and on the other side, by the close contacts of OC−H···N_{Ar} [$d_{N···H}$ ($\angle$)=3.47 Å (107.3°)] and C−H···C_{Ar} (3.04−3.82 Å, π-centroid···H−C distance 3.19 Å). As shown in Fig. 2 (insert box), binding of adjacent molecular sheets is attained by means of arene−arene interactions via double C−H···N_{Ar} close contacts [$d_{N···H}$ ($\angle$)=2.91 Å (158.7°), 3.05 Å (168.8°)] between solvated and non-solvated quinoxaline rings, which are arranged in antiparallel manner and separated by an intercentroid distance of 6.68 Å.[25] The association is secured by a OCH_3 group exerting one OC−H···N_{Ar} hydrogen bond to each of the linked quinoxaline rings [$d_{N···H}$ ($\angle$)=2.62 Å (166.5°) and 2.80 Å (131.0°)].

The C_2-symmetric quadruple-bridged [6,4]orthocyclophane **D2a** deposited as a racemic mixture composed of *P*- and *M*-forms from CH_2Cl_2/EtOH solution in the orthorhombic space group *Pca2* (1). Fig. 3a shows the arrangement of molecular aggregates viewed along *a*-axis on *bc*-plane that are composed of wave-like columns of **D2a** molecules. The wave-like molecular column of **D2a** is constructed by means of arene−arene interactions between quinoxaline rings of adjacent molecules having opposite chirality, which assume the parallel-displaced geometry[25] as shown in Fig. 3b (viewed along *c*-axis). They are separated by an intercentroid distance of 6.48 Å with a dihedral angle of about 180°, and linked by double, nearly linear C−H···N_{Ar} hydrogen bonds [$d_{N···H}$ ($\angle$)=2.70 Å (6.7°) and 2.66 Å (5.4°), Table 1]. This offset parallel structure is further stabilized by $OCH_3···\pi$ interactions exerted by the polar OCH_3 groups of **D2a** concurrently located close to the quinoxaline ring of two adjoining molecules of **D2a** with $d_{H···\pi}$ distances of 2.54−6.32 Å (π-centroid···H−C distance 4.19 Å) and 3.26−7.18 Å (π-centroid···H−C distance 5.05 Å).

Examination of the crystal packing (Fig. 3a,c, and Table 1) further reveals that the binding forces between molecular columns are mainly presented by the polar OCH_3 groups using OC−H···O hydrogen bonds [$d_{O···H}$ ($\angle$)=2.57 Å (34.5°), 2.79 Å (40.0°)] and $OCH_3···\pi$ interactions resulting from C−H···N_{Ar} and C−H···C_{Ar} close contacts with H···N_{Ar} and π-centroid···H distances within the ranges of 2.9−3.5 Å and 3.1−3.8 Å, respectively.

The racemic quadruple-bridged [6,4]orthocyclophane **D2f** co-crystallized with molecules of $CHCl_3$ in the monoclinic space group $C2/c$. Resembling **D2a** in molecular skeleton, but annelated by aryl ring, that is, of more capability for π−π stacking interaction, molecules of **D2f** employ two types of arene−arene interaction between benzoquinoxaline rings to construct molecular columns as illustrated in Fig. 4a. Each molecular column is composed of arrays of wave-like molecular strips (Fig. 4b). Similar to that used by **D2a**, one arene−arene interaction adopts offset parallel structure (left, Fig. 4),[25] in which benzoquinoxaline rings of adjacent molecules of homochiral **D2f** are separated by a centroid-to-centroid distance of

Table 1
Selected packing motifs in the crystal structures involving aryl and methoxy groups[a]

	Arene−arene interaction				OCH₃···π interaction			OMe···OMe
	mold[b]	Shortest interatomic distance		ArH···N_Ar H-bond or close contact	Hydrogen bond or close contact			
					OC−H···N_Ar	OC−H···(C/N)_Ar	C_Ar−H···O	OC−H···O
		$d_{C\cdots N}$	$d_{C\cdots C}$	$d_{N\cdots H}$ (∠)	$d_{N\cdots H}$ (∠)	$d_{C\cdots H}$ ()[c]	$d_{O\cdots H}$ (∠)	$d_{O\cdots H}$ (∠)
D1a	Δ (6.57)	3.59	3.59	2.73 (155.0)	2.80 (131.0)	2.83−4.51 (3.07)		2.74 (148.7)
	◇ (6.68)			2.91 (158.7)	3.47 (107.3)	3.04−3.82(3.19)		2.78 (157.8)
				3.05 (168.8)	2.62 (166.5)			
D2a	◇ (6.48)	3.65	4.24	2.70 (6.7)	2.98 (131.7)	2.54−6.32 (4.19)		2.57 (34.5)
				2.66 (5.4)	3.21 (114.2)	3.26−7.18 (5.05)		2.79 (40.0)
					3.48 (86.1)	2.98−5.47 (3.77)		
						3.21−5.22 (3.71)		
						3.04−4.42 (3.15)		
D2f	◇ (6.92)	4.08	4.15	3.15 (176.4)		3.11−9.13(5.81)		
	□ (5.27)	4.50	3.54	4.00 (122.7)		3.12−7.44(4.55)		
D3f	□ (3.87)	3.38	3.41	3.42 (79.5)		2.74−5.80 (3.16)	2.64 (139.5)	
	□ (4.03)	3.45	3.58	3.40 (85.3)		3.02−6.44 (3.63)	2.66 (138.6)	
D2g-α	□ (4.25)	3.30	3.38	3.52 (105.6)	3.16 (124.2)	3.16−6.60(4.65)	2.77 (156.5)	
	□ (3.85)	3.47	3.44	3.28 (82.9)	3.52 (127.7)	3.51−6.30 (4.74)	2.96 (125.7)	
				3.54 (78.1)				
				3.37 (89.7)				
D3g-α	Δ (5.85)	3.52		2.62(163.4)		3.17−5.91 (4.15)		
		3.60		3.32 (99.9)	2.93 (138.8)	2.93−5.26 (3.67)		
	◇ (7.23)	3.48		2.55 (170.5)	2.93 (105.8)	2.76−5.47 (3.62)		
		3.83		3.09 (137.4)	2.78 (125.1)	2.78−6.17 (4.29)	2.98 (134.1)[d]	
	Δ (4.88)[d]	3.93	3.89[d]	3.30 (126.8)[d]		2.74−6.21 (4.17)	3.07 (147.2)[d]	

[a] Distances (d) are in Å unit and angles (∠) shown in parentheses are in degree unit (°).
[b] Structure of alignment for arene rings with centroid-to-centroid distance shown in parentheses: (△) edge-to-face, herringbone (face-tilted-T) geometry; (◇) offset parallel (parallel-displaced) geometry; (□) face-to-face, parallel, π−π stacking geometry.
[c] The distances of hydrogen atom to all carbon/nitrogen atoms of aryl ring with H-to-centroid distance shown in parentheses.
[d] The interaction involving spacer tetrahydronaphthalene ring of **D3f** and **D3g-α**.

Table 2
Selected packing motifs in the crystal structures involving solvate molecules[a,b]

| | Solvate | Cl−C−H···N_Ar or H−C−Cl···H H-bond and close contact | | | |
		C−H···N_Ar	Ar−H···Cl	Cl···H−CO	C−H···Cl_Bridgehead
D1a	CH₂Cl₂	2.49 (140.9)	3.51 (108.5)		
D2f	CHCl₃	2.47 (146.7)	3.12 (134.9)	3.06 (111.1)	3.16 ()
				3.02 (118.6)	
D3f	CHCl₃	2.61 (142.2)	2.98 (161.6)	3.06 (105.4)	3.34 (123.9)
			3.32 (137.0)	3.27 (92.0)	
		2.49 (144.5)	3.10 (155.3)	3.28 (116.7)	3.02 (130.1)
			3.15 (135.3)		
			3.19 (121.8)		
			3.28 (147.9)		
			3.12 (154.5)		
D3g-α	CHCl₃	2.44 (151.1)	3.44 (112.6)	2.94 (118.3)	
		2.54 (149.3)	3.27 (136.1)[c]	3.90 (116.2)	
				3.09 (162.9)	

[a] **D2a** and **D2g-α** did not crystallize with solvate molecules.
[b] Distances (d) are in Å unit and angles (∠) shown in parentheses are in degree unit (°).
[c] The interaction involving spacer tetrahydronaphthalene ring of **D3g-α**.

6.92 Å with dihedral angle of about 180° and are allied by symmetrical, double ArH···N_Ar close contacts [$d_{N\cdots H}$ (∠)=3.15 Å (176.4°)]. This packing motif is further supported by the OCH₃···π close contacts (3.11−9.13 Å, π-centroid···H−C distance 5.81 Å). The other arene−arene interaction assumes parallel, face-to-face, stacking geometry[26] with a centroid-to-centroid distance of 5.27 Å and shortest interplanar carbon-to-carbon distances of 3.54 Å between benzoquinoxaline rings of heterochiral **D2f** (right, Fig. 4). Interestingly as shown in Fig. 4 and Table 2, the solvating CHCl₃ are sited between molecular columns of **2Df** and each one of them is attached to one benzoquinoxaline ring by making use of Cl₃C−H···N_Ar hydrogen bond [$d_{N\cdots H}$ (∠)=2.47 Å (146.7°)], and Cl₃C−H···Cl_Bridgehead, C_Ar−H···Cl, and OC−H···Cl close contacts [$d_{Cl\cdots H}$ (∠)=3.16 Å (129.5°), $d_{Cl\cdots H}$ (∠)=3.12 Å (134.9°), and $d_{Cl\cdots H}$ (∠)=3.06 Å (111.1°), respectively]. Worth of notice is that CHCl₃

molecule places its acidic hydrogen atom within the distance range of forming hydrogen bonds to concurrently link up with electron-rich nitrogen and chlorine atoms (Fig. 4b). Through collaboration with the polarized OCH₃ group, CHCl₃ molecules are also responsible for stabilizing the association of molecular columns of **D2f** by grabbing nearby homochiral molecules of **D2f** via OC−H···Cl close contact [$d_{Cl\cdots H}$ (∠)=3.02 Å (118.6°)]. The association of molecular columns is also found to be stabilized by the OCH₃···π close contacts between **D2f** of heterochirality (3.12−7.44 Å, π-centroid···H−C distance 4.55 Å), Fig. 4a.

Fig. 5 illustrates the packing motifs observed for single crystal of quadruple-bridged [6,4]orthocyclophane **D3f** obtained from CHCl₃ solution in the triclinic space group *P*1. Bearing benzoquinoxaline rings similar to **D2f**, a molecule of **D3f** operates bilateral connection with its enantiomeric neighbors to form wave-like molecular strip
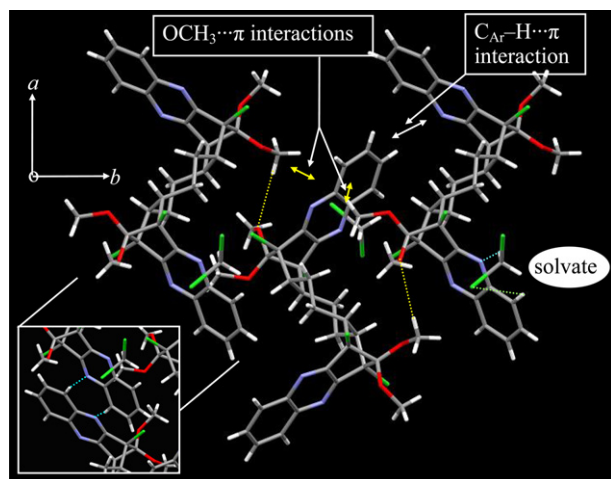
Fig. 2. The packing motifs observed for crystal **D1a** viewed along *c*-axis on *ab*-plane, showing molecular sheet assembled mainly by using the motifs of C_{Ar}–H···π and OCH$_3$···π interactions. Insert shows double H···N hydrogen bonds (cyan dotted line) connecting two molecules of **D1a** in adjacent molecular sheets. In this and successive figures, unless otherwise specified, the packing motifs are denoted by symbol and color as following: white double-headed arrow for arene-arene interaction, yellow double-headed arrow for OCH$_3$···π interaction, cyan dotted line for C_{Ar}–H···N$_{Ar}$, OC–H···N$_{Ar}$, and ClC–H···N$_{Ar}$, yellow dotted line for C_{Ar}–H···O and OC–H···O, and green dotted line for C_{Ar}–H···Cl, OC–H···Cl, and C–H···Cl$_{Bridgehead}$ hydrogen bond or close contact. Color coding for atom: C, gray; H, white; N, blue; O, red; Cl, green. Distances (d) and angles (∠) are listed in Tables 1 and 2.

in the crystal, taking advantage of direct π−π interaction between benzoquinoxaline rings in face-to-face, parallel-stacked structure. Both structures of arene–arene interaction are reinforced by the polarized OMe groups via C_{Ar}–H···O hydrogen bonds [d$_{O···H}$ (∠)= 2.64 Å (139.5°), 2.66 Å (138.6°)]. Interestingly, the configuration of π−π stacked interactions at the two sides are different in the centriod-to-centriod distance (3.87 Å vs 4.03 Å), the shortest interplanar distance (d$_{C···N}$: 3.38 Å vs 3.45 Å), and the striking feature of solvation. As shown in Fig. 5b (left), the solvating CHCl$_3$ molecules discriminatingly bind only one of the two benzoquinoxaline rings in **D2f** by tripodal style using C–H···N$_{Ar}$ hydrogen bonds [d$_{N···H}$ (∠)=2.49 Å (144.5°), 2.61 Å (142.2°)], and two C_{Ar}–H···Cl close contacts [d$_{Cl···H}$ (∠)=2.98 Å (161.1°)/3.32 Å (137.0°), 3.10 Å (155.3°)/3.15 Å (135.3°)]. The molecule of CHCl$_3$ is thus positioned and oriented such that its hydrogen atom is also brought into closely contact with the bridgehead chlorine atom of **D3f** [d$_{Cl···H}$ (∠)=3.02 Å (130.1°), 3.34 Å (123.9°)].[1b,24] Two CHCl$_3$-affixed benzoquinoxaline rings then assemble to form a 'dimer' of **D2f** via π−π stacking interactions. Furthermore, the solvating CHCl$_3$ appear to play a key role in sustaining the association of molecular strips of **D3f**, as close contacts with nearby molecules of **D3f** by motifs of C_{Ar}–H···Cl [d$_{Cl···H}$ (∠)=3.28 Å (147.9°), 3.12 Å (154.5°)] and OC–H···Cl [d$_{Cl···H}$ (∠)=3.06 Å (105.4°), 3.27 Å (92.0°), 3.28 Å (116.7°)] were observed as well, as shown in Fig. 5b (right). Additional forces of supporting association of molecular strips derived from the interactions of the polarized OMe groups with benzoquinoxaline via the OCH$_3$···π close contacts (2.74−5.80 Å, π-centroid···H−C distance 3.16 Å; 3.02−6.44 Å, π-centroid···H−C distance 3.63 Å) and fused-benzene rings (intercalator) via C_{Ar}–H···O hydrogen bonding [d$_{O···H}$ (∠)=2.94 Å (156.1°)], Fig. 5a.

The packing motifs observed for crystal of pyridopyrazine ring-walled quadruple-bridged [6,4]orthocyclophane **D2g**-α (monoclinic space group *P*2(1)/*c*) is shown in Fig. 6. The association of **D2g**-α to form wave-like molecular strips is predominantly achieved by π−π interactions between parallel-stacked pyridopyrazine rings. Similar to those observed in the crystal of **D3f**, the π−π stacking interactions in the crystal of **D2g**-α also adopt two

different configurations with centriod-to-centriod distances of 4.25 Å and 3.85 Å, and shortest interplanar distances (d$_{C···N}$) of 3.30 Å and 3.47 Å, respectively. Both structures of arene–arene interaction are reinforced by the polarized OMe groups via C_{Ar}–H···O hydrogen bonds [d$_{O···H}$ (∠)=2.77 Å (156.5°), 2.96 Å (125.7°), Table 1]. Alliance between molecular strips is mainly endowed with OCH$_3$···π close contacts (3.16−6.60 Å, π-centroid···H−C distance 4.65 Å; 3.51−6.30 Å, π-centroid···H−C distance 4.74 Å). Interestingly, in this alliance a bridgehead chlorine atom is very near to the cyclohexene ring (intercalator) of adjacent **D2g**-α to express =C–H···Cl hydrogen bonds [d$_{Cl···H}$ (∠)=2.93 Å (116.5°)/2.99 Å (117.1°)], further locking molecular strips together, Fig. 6.

The quadruple-bridged [6,4]orthocyclophane **D3g**-α co-crystallized with molecules of CHCl$_3$ in the monoclinic space group *P*2(1)/ *c*. Although having pyridopyrazine-ring sidewalls as **D2g**-α, the crystal of **D3g**-α employs the mode of C_{Ar}–H···π interactions, instead of π−π stacking interactions, for associating molecules of **D3g**-α. Fig. 7a depicts enantiomeric pairs of **D2g**-α aligning to form molecular arrays viewed along *c*-axis, which clearly show their association with the assist of C_{Ar}–H···π interactions by means of double N···H close contacts [d$_{N···H}$ (∠)=2.55 Å (170.5°)/3.09 Å (137.4°)] with a centriod-to-centriod distance of 7.32 Å between pyridopyrazine rings, and is reinforced by OCH$_3$···π interactions [2.78−6.17 Å, π-centroid···H−C distance 4.29 Å with OCH···N hydrogen bond (d$_{N···H}$ (∠)=2.78 Å (125.1°)); 2.74−6.21 Å, π-centroid···H−C distance 4.17 Å] and C_{Ar}–H···O close contacts [d$_{N···H}$ (∠)=3.07 Å (147.2°)] between the methoxyl oxygen atom and a hydrogen atom of fused-benzene rings (intercalator), as shown in Fig. 7b. The molecular array of **D3g**-α is constructed predominantly by a three-component C_{Ar}–H···π interaction between two pyridopyrazine rings and the fused-benzene rings of intercalator, separated by centriod-to-centriod distances of 5.85 Å, 4.88 Å, and 4.57 Å, respectively (Fig. 7b, Table 1). Pyridopyrazine rings are connected using interactions of double N···H close contacts [d$_{N···H}$ (∠)=2.62 Å (163.4°)/3.32 Å (99.9°)], while intermolecular interaction between pyridopyrazine and fused-benzene rings is presented by N···H close contact [d$_{N···H}$ (∠)=3.30 Å (126.8°)]. In this packing motif, OMe groups are located close to pyridopyrazine ring to apply OCH$_3$···π interactions[2.93−5.26 Å, π-centroid···H−C distance 3.67 Å, with OCH···N hydrogen bond (d$_{N···H}$ (∠)=2.93 Å (105.8°)); 3.17−5.91 Å, π-centroid···H−C distance 4.15 Å], and the fused-benzene ring to exert C_{Ar}–H···O hydrogen bond [d$_{O···H}$ (∠)= 2.98 Å (134.1°)], further sustain the structure. Examination of crystal packing reveals that the solvate molecule of CHCl$_3$ appears to be entrapped in the cavity formed by four molecules of **D3g**-α (Fig. 7c and Table 2), and to act as binding agent for connecting adjacent molecular arrays to construct 3D-network of crystal structure.

3. Conclusion

In summary, we have synthesized multi-bridged [n,n']orthocyclophanes encompassing two sidewalls (phane parts) oriented in opposite direction and made of quinoxaline, 6,7-disubstituted quinoxaline, benzoquinoxaline or pyrido[2,3-*b*]pyrazine rings by a three-step synthetic route outlined in Scheme 1. The synthesis starts with three bis-Diels–Alder adducts and subsequently involves the ruthenium-promoted oxidation and condensation of the resulting bis-α-diketones with various arene-1,2-diamines to furnish nineteen Z-shaped quadruple-bridged [6,6] and [6,4]orthocyclophanes, demonstrating the versatility and efficacy of the synthetic method. Among the synthesized orthocyclophanes we obtained single crystals of **D1a**, **D2a**, **D2f**, **D3f**, **D2g**-α, and **D3g**-α and examined their crystal structure and packing. Arene–arene interactions between *N*-containing arene rings, in modes of
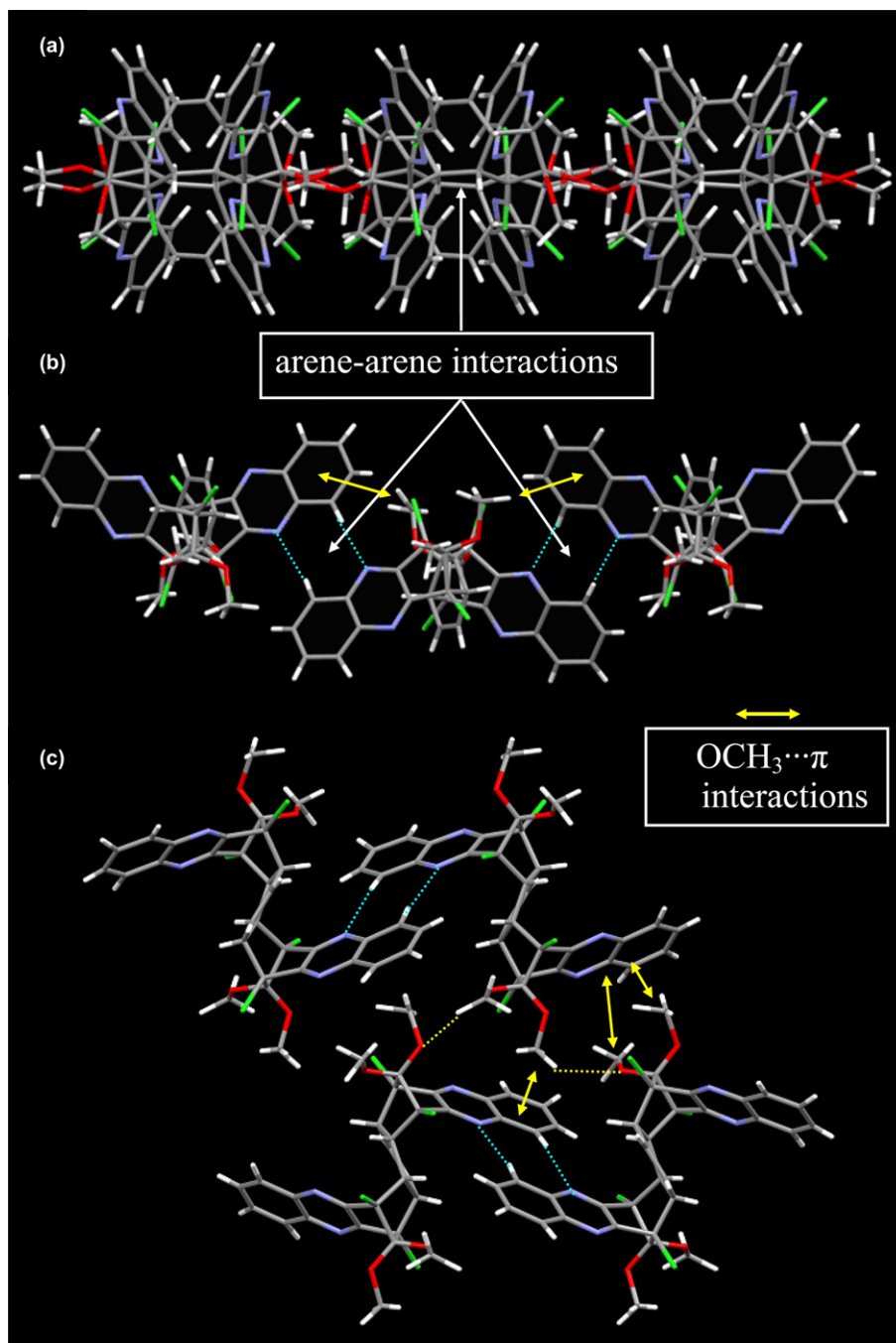
Fig. 3. The packing motifs observed for crystal **D2a**. (a) view along *a*-axis showing the alignment of molecular columns on *bc*-plane (b) view along *c*-axis showing the packing motifs of assembling a wave-like molecular column on *ab*-plane. (c) view along *b*-axis showing the packing motifs of binding between molecular columns on *ca*-plane.

C_{Ar}–H···π interaction with face-tilted-T (**D1a** and **D3g-α**) or parallel-displaced geometry (**D1a**, **D2a**, **D2f**, and **D3g-α**) and face-to-face, π–π stacking interaction (**D2f**, **D3f**, and **D2g-α**), were observed as the major driving force for molecular assembly and crystal packing. In the packing motif of C_{Ar}–H···π interaction, nitrogen atoms at heteroaromatic ring often play significant role through arrangement of double ArH···N_{Ar} hydrogen bonding or close contact. Additional noncovalent interactions involving the C–H bond or oxygen atom of polar OCH_3 group and the solvate $CHCl_3$ molecule with its acidic H and high electronegative Cl, which are attributed cooperatively to the formation of three-dimensional crystalline architectures in the crystals, were also disclosed. In

combination, these results suggest that design and synthesis of quinoxaline-based multi-bridged orthocyclophanes that have potential of building up complex crystalline architectures taking advantage of these noncovalent interactions could be realized by synthetic strategy shown in Scheme 1.

4. Experimental section

4.1. General (see **Supplementary data**)

*4.1.1. General procedure for the preparation of bis-α-diketones **C**.* A suspension of $NaIO_4$ (2.50 mmol) and $RuCl_3 \cdot 3H_2O$ (0.11 mmol) in
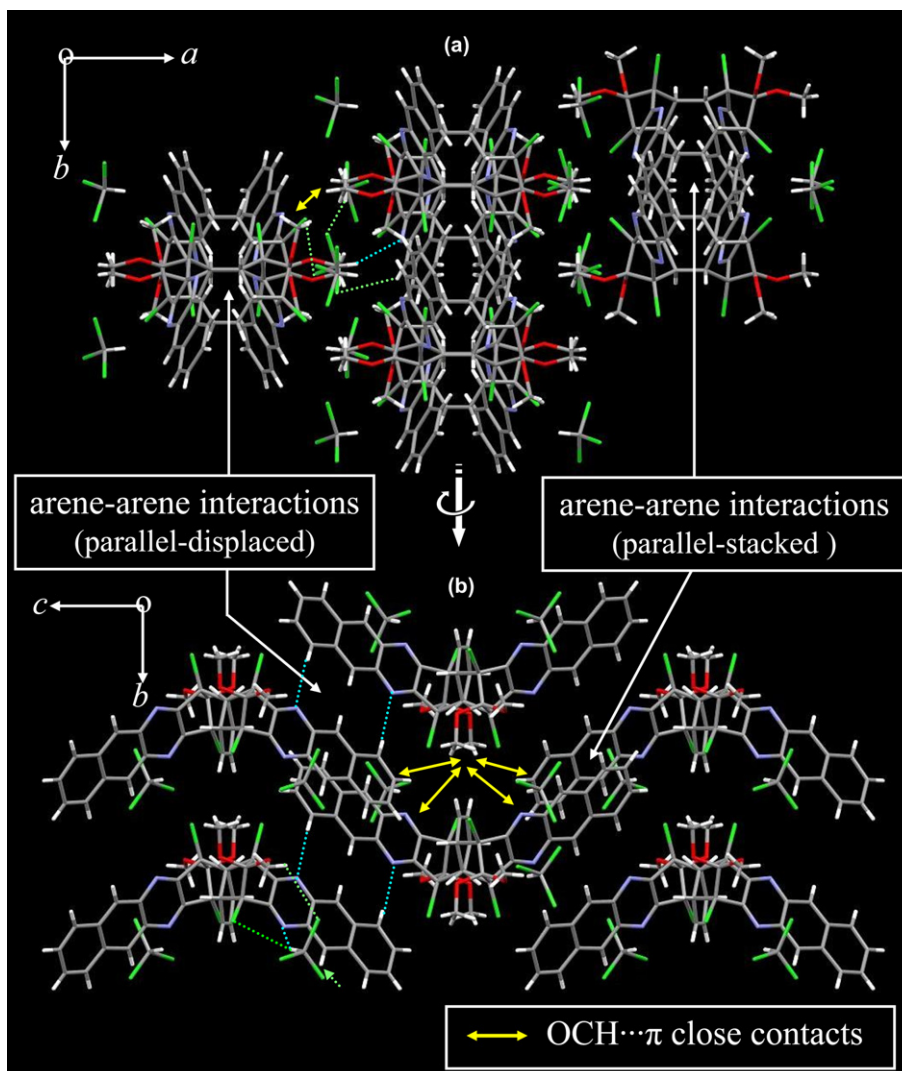
Fig. 4. The packing motifs observed for crystal **D2f** with solvating CHCl$_3$. (a) The arrangement of molecular columns on *ab*-plane viewed along *c*-axis. The association between molecular columns is mediated by solvating molecules. (b) The middle molecular column shown in (a) is viewed along *a*-axis on *bc*-plane to show the association of molecules of **D2f** by the parallel-displaced $\pi-\pi$ interaction, and the parallel-stacked $\pi-\pi$ interaction.

water (3.4 mL) was added in portions to an ice-cooled suspension of bis-DA-adduct **B1**,[13] **B2**,[15] **or B3**[14] (1.0 mmol) in CHCl$_3$ (10 mL) and CH$_3$CN (10 mL) over a period of hours, monitored by TLC and ^{1}H NMR. After the reaction was completed, the mixture was added water (50 mL) and extracted with CHCl$_3$ (2×15 mL). The combined organic phase was washed with water (2×20 mL), dried over MgSO$_4$, and evaporated. Purification by recrystallization from CHCl$_3$ afforded yellow platelets of bis-α-diketone **C**. In some cases, the reaction mixture was filtered directly to give a residue, which was washed with CH$_3$CN (2×30 mL) and purified via recrystallization.

*4.1.1.1. (1α,2β,5α,6β,9β,10α,13β,14α)-1,6,9,14-Tetrachloro-17,17,18,18-tetramethoxypentacyclo [12.2.1.1^{6,9}.0^{2,13}.0^{5,10}]octadecane-7,8,15,16-tetraone (**C1**).* Reaction time 72 h, yield 84%. Mp 294–296 °C (decomp.); IR (KBr) 2991 (m), 2951 (m), 2905 (m), 2847 (m), 1794 (s), 1766 (s), 1468 (s), 1287 cm^{-1} (s); ^{1}H NMR (400 MHz, CDCl$_3$) δ 3.69 (s, 6H), 3.52 (s, 6H), 2.82 (d, *J*=10.2 Hz, 4H), 2.08 (d, *J*=11.6 Hz, 4H), 0.76 (m, 4H); MS (FAB) 564 (3) [M+8]$^+$, 556 (7) [M]$^+$; 154 (100). Anal. Calcd for C$_{22}$H$_{24}$Cl$_4$O$_8$ (558.23): C, 47.33; H, 4.33; O, 22.93; found: C, 47.23; H, 4.66; O, 22.53.

4.1.1.2. (1α,2β,3α,4β,7β,8α,11β,12α)-1,4,7,12-Tetrachloro-15,15,16,16-tetramethoxypentacyclo [10.2.1.1^{4,7}.0^{2,11}.0^{3,8}]hexadecane-

9-ene-5,6,13,14-tetraone (**C2**). Reaction time 12 h, yield 95%. Mp 295–298 °C (decomp.); IR (KBr) 3003 (m), 2954 (s), 2845 (m), 1810 (s), 1793 (s), 1771 (s), 1456 (s), 1216 cm^{-1} (s); ^{1}H NMR (400 MHz, CDCl$_3$) δ 5.74 (d, *J*=1.0 Hz, 2H), 3.76 (s, 6H), 3.54 (s, 6H), 3.13 (d, *J*=5.6 Hz, 2H), 3.03 (d, *J*=5.6 Hz, 2H); ^{13}C NMR (100 MHz, CDCl$_3$) δ 188.3 (s), 186.2 (s), 124.7 (d), 101.9 (s), 78.8 (s), 78.6 (s), 52.9 (q), 52.3 (q), 39.9 (d), 36.0 (d); MS (FAB) 529 (w) [M+5]$^+$, 527 (w) [M+3]$^+$, 154 (100). Anal. Calcd for C$_{20}$H$_{18}$Cl$_4$O$_8$ (528.16): C, 45.48; H, 3.44; O, 24.23; found: C, 45.42; H, 3.34; O, 24.52.

*4.1.1.3. (1α,2β,3α,4β,7β,8α,15β,16α)-1,4,7,16-Tetrachloro-19,19,20,20-tetramethoxyhexacyclo [14.2.1.1^{4,7}.0^{2,15}.0^{3,8}.0^{9,14}]icosane-9(14),10,12-triene-5,6,17,18-tetraone (**C3**).* Reaction time 12 h, yield 98%. Mp 287–288 °C (decomp.); IR (KBr) 2995 (w), 2954 (m), 2848 (m), 1802 (s), 1770 (s), 1466 (m), 1230 cm^{-1} (s); ^{1}H NMR (400 MHz, CDCl$_3$) δ 7.54 (dd, *J*=6.4, 3.5 Hz, 2H), 7.29 (dd, *J*=6.4, 3.5 Hz, 2H), 3.81 (s, 6H), 3.79 (d, *J*=12.5 Hz, 2H), 3.53 (s, 6H), 3.52 (d, *J*=12.5 Hz, 2H); ^{13}C NMR (100 MHz, CDCl$_3$) δ 188.6 (s), 185.1 (s), 129.7 (d), 128.5 (d), 126.8 (s), 101.8 (s), 80.9 (s), 79.0 (s), 52.9 (q), 52.4 (q), 42.1 (d), 36.9 (d); MS (FAB) 579 (2) [M+5]$^+$, 577 (1) [M+3]$^+$, 154 (100). Anal. Calcd for C$_{24}$H$_{20}$Cl$_4$O$_8$ (578.22): C, 49.85; H, 3.49; O, 22.14; found: C, 49.60; H, 3.51; O, 22.34.
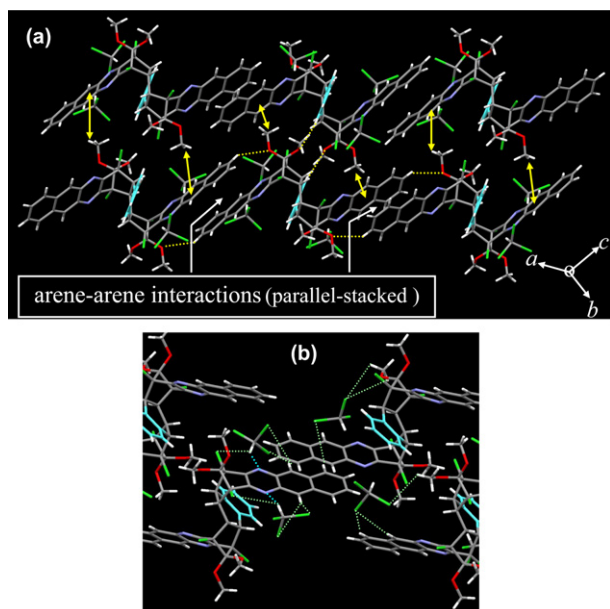
Fig. 5. The packing motifs observed for crystal **D3f** with solvating CHCl$_3$. (a) A molecule of **D3f** operates bilateral connection to form molecular array with its enantiomers using two face-to-face, parallel-stacked π–π interactions having different centriod-to-centriod distances and status of salvation. Inter-array association is attained mainly by OCH$_3$···π close contacts. (b) The face-to-face, parallel-stacked π–π interaction between pairs of CHCl$_3$-attached benzoquinoxaline rings showing the involvement of molecule of CHCl$_3$ intermolecular association. The benzene ring of spacer tetrahydronaphthalene in **D3f** is cyan colored.

4.1.2. General procedure for the preparation of symmetric bis-quinoxalines C. Into a solution of bis-α-diketone **C** (0.50 mmol) in chlorobenzene (12.5 mL) containing a catalytic amount of zinc acetate was added o-phenylenediamine (1.10 mmol) under reflux for hours, monitored by TLC and ^{1}H NMR. The reaction mixture was filtered to remove salt and the filtrate was concentrated. The residue was purified via recrystallization from EtOH/CHCl$_3$ (3/2 by vol) to afford pure adduct.

4.1.2.1. (1α,2β,5α,6β,17β,18α,21β,22α)-8,15,24,31-Tetraaza-1,6,17,22-tetrachloro-33,33,34,34-   tetramethoxynonacyclo[20.10.1.1.^{16,17}.0^{2,21}.0^{5,18}.0^{7,10}.0^{9,14}.0^{23,32}.0^{25,30}]tetratriacontane-7(10),8,10,12,14,23(32),24,26,28,30-decaene (D1a). Reaction time 8 h, yield 94%. Mp 318–321 °C (decomp.); IR (KBr) 3089 (w), 2942 (s), 2926 (s), 2902 (m), 2839 (m), 1511 (s), 1463 (s), 1199 cm^{-1} (s); ^{1}H NMR (400 MHz, CDCl$_3$) δ 8.23 (dd, J=6.2, 3.4 Hz, 4H), 7.81 (dd, J=6.2, 3.4 Hz, 4H), 3.63 (s, 6H), 3.34 (s, 6H), 2.71 (d, J=10.2 Hz, 4H), 2.10 (d,
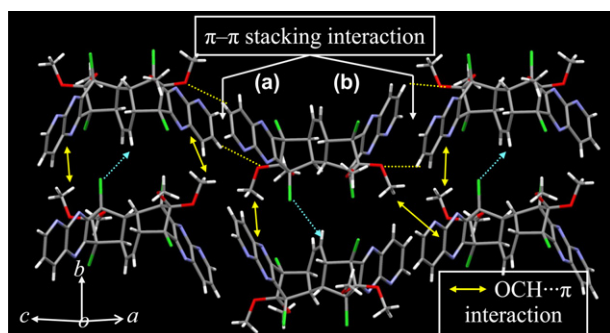

Fig. 6. The packing motifs observed for crystal **D2g-α** showing two molecular bands formed by two types of π–π interaction between parallel-stacked pyridopyrazine rings with (a) a centriod-to-centriod distance of 4.25 Å and (b) a centriod-to-centriod distance of 3.85 Å. Alliance between molecular bands is mainly endowed with OCH$_3$···π interaction and =C–H···Cl hydrogen bonds [d$_{Cl···H}$ (∠)=2.93 Å (116.5°)/2.99 Å (117.1°)], cyan dotted arrow].
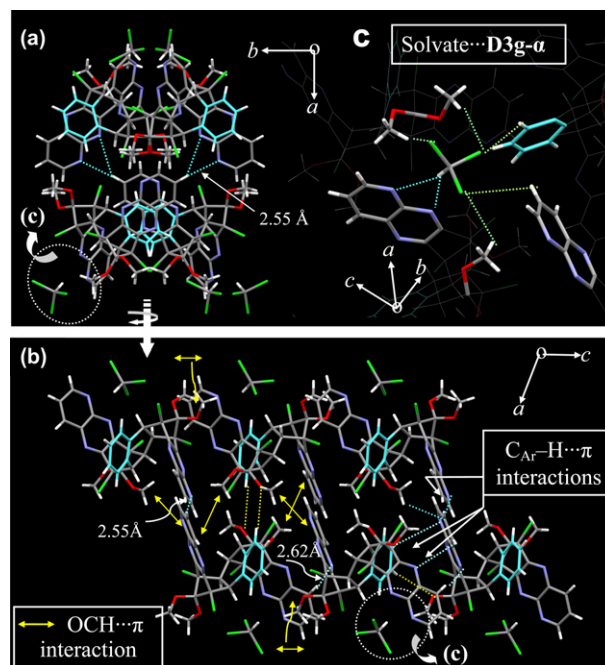

Fig. 7. The packing motifs observed for crystal **D3g-α** and solvating CHCl$_3$. (a) Cross sections of two molecular arrays, each formed by enantiomeric pair on ab-plane viewed along c-axis. (b) Molecular arrays on ac-plane viewed along b-axis by rotating (a) 90°. (c) The formation of CHCl$_3$@**D3g-α**, in which the CHCl$_3$ molecule entrapped in the cavity formed by four molecules of **D3g-α**.

J=11.6 Hz, 4H), 0.07 (dd, J=10.2, 9.6 Hz, 4H); ^{13}C NMR (100 MHz, CDCl$_3$) δ 152.6 (s), 142.4 (s), 129.8 (d), 129.4 (d), 110.3 (s), 75.9 (s), 52.3 (q), 51.9 (q), 49.5 (d), 22.1 (t); MS (FAB) 707 (8) [M+H+6]$^+$, 705 (22) [M+H+4]$^+$, 703 (42) [M+H+2]$^+$, 701 (31) [M+H]$^+$, 154 (100); UV/vis (CHCl$_3$) λ$_{abs}$ (ϵ) 244, 318, 330 nm (70,453 mol^{-1} dm^3 cm^{-1}). Emission (CHCl$_3$) λ$_{em}$ 390 nm. Anal. Calcd for C$_{34}$H$_{32}$Cl$_4$N$_4$O$_4$: C, 58.13; H, 4.59; N, 7.98; O, 9.11; found: C, 58.22; H, 4.49; N, 7.92; O, 9.10.

4.1.2.2. (1α,2β,5α,6β,17β,18α,21β,22α)-8,15,24,31-Tetraaza-1,6,17,22-tetrachloro-33,33,34,34-tetramethoxy-11,12,27,28-tetramethylnonacyclo[20.10.1.1.^{16,17}.0^{2,21}.0^{5,18}.0^{7,10}.0^{9,14}.0^{23,32}.0^{25,30}]tetratriacontane-7(10),8,10,12,14,23(32),24,26,28,30-decaene (D1b). Reaction time 8 h, yield 94%. Mp>300 °C; IR (KBr) 2983 (w), 2949 (s), 2839 (m), 1499 (s), 1194 cm^{-1} (s); ^{1}H NMR (400 MHz, CDCl$_3$) δ 7.98 (s, 4H), 3.61 (s, 6H), 3.33 (s, 6H), 2.65 (d, J=10.2 Hz, 4H), 2.51 (s, 12H), 2.06 (d, J=11.6 Hz, 4H), 0.02 (dd, J=10.2, 9.6 Hz, 4H); ^{13}C NMR (100 MHz, CDCl$_3$) δ 151.6 (s), 141.0 (s), 140.3 (s), 128.6 (d), 110.3 (s), 75.9 (s), 52.2 (q), 51.8 (q), 49.6 (d), 22.1 (t), 20.3 (q); MS (FAB) 764 (1) [M+8]$^+$, 762 (2) [M+6]$^+$, 760 (6) [M+4]$^+$, 758 (7) [M+2]$^+$, 756 (2) [M]$^+$, 154 (100); UV/vis (CHCl$_3$): λ$_{abs}$ (ϵ) 253, 328, 343 nm (65,574 mol^{-1} dm^3 cm^{-1}). Emission (CHCl$_3$) λ$_{em}$ 380 nm. HRMS (FAB) calcd for C$_{38}$H$_{41}$Cl$_4$N$_4$O$_4$ [M+H]$^+$: 757.1882; found: 757.1889.

4.1.2.3. (1α,2β,5α,6β,17β,18α,21β,22α)-8,15,24,31-Tetraaza-1,6,17,22-tetrachloro-11,12,27,28, 33,33,34,34-octamethoxynonacyclo[20.10.1.1.^{16,17}.0^{2,21}.0^{5,18}.0^{7,10}.0^{9,14}.0^{23,32}.0^{25,30}]tetratriacontane-7(10),8,10,12,14,23(32),24,26,28,30-decaene (D1c). Reaction time 8 h, yield 92%. Mp>300 °C; IR (KBr) 2948 (s), 2844 (m), 1631 (m), 1504 (s), 1469 (s), 1430 (s), 1244 cm^{-1} (s); ^{1}H NMR (400 MHz, CDCl$_3$) δ 7.54 (s, 4H), 4.06 (s, 12H), 3.61 (s, 6H), 3.33 (s, 6H), 2.67 (d, J=10.2 Hz, 4H), 2.07 (d, J=11.6 Hz, 4H), 0.04 (dd, J=10.2, 9.6 Hz, 4H); ^{13}C NMR (100 MHz, CDCl$_3$) δ 152.3 (s), 149.9 (s), 139.1 (s), 110.7 (s), 107.5 (d), 76.0 (s), 56.5 (q), 52.2 (q), 51.8 (q), 49.8 (d), 22.1 (t); MS (FAB) 828 (5) [M+8]$^+$, 826 (18) [M+6]$^+$, 824 (26) [M+4]$^+$, 822 (29) [M+2]$^+$, 820 (7) [M]$^+$, 64 (100); UV/vis (CHCl$_3$) λ$_{abs}$ (ϵ) 248, 359 nm (28,145 mol^{-1} dm^3 cm^{-1}). Emission (CHCl$_3$) λ$_{em}$ 381 nm. HRMS

(FAB) calcd for $C_{38}H_{41}Cl_4N_4O_8$ [M+H]$^+$: 821.1653; found: 821.1666. Anal. Calcd for $C_{38}H_{40}Cl_4N_4O_8$: C, 55.49; H, 4.90; N, 6.81; O, 15.56; found: C, 55.39; H, 4.69; N, 6.73; O, 15.38.

4.1.2.4. (1α,2β,5α,6β,17β,18α,21β,22α)-8,15,24,31-Tetraaza-1,6,11,12,17,22,27,28-octachloro-33,33,34,34-tetramethoxynonacyclo [20.10.1.1.^{16,17}.0^{2,21}.0^{5,18}.0^{7,10}.0^{9,14}.0^{23,32}.0^{25,30}]tetratria-contane-7 (10),8,10,12,14,23(32),24,26,28,30-decaene (D1d). Reaction time 12 h, yield 92%. Mp>300 °C; IR (KBr) 3078 (w), 3065 (w), 3006 (m), 2984 (m), 2949 (s), 2907 (m), 2842 (m), 1481 (s), 1197 cm^{-1} (s); ^{1}H NMR (400 MHz, CDCl$_3$) δ 8.34 (s, 4H), 3.63 (s, 6H), 3.34 (s, 6H), 2.71 (d, J=10.2 Hz, 4H), 2.08 (d, J=11.6 Hz, 4H), 0.02 (dd, J=10.2, 9.6 Hz, 4H); ^{13}C NMR (100 MHz, CDCl$_3$) δ 153.8 (s), 141.0 (s), 134.5 (s), 130.1 (d), 110.2 (s), 75.8 (s), 52.4 (q), 52.0 (q), 49.5 (d), 22.1 (t); UV/vis (CHCl$_3$) λ$_{abs}$ (ε) 249, 344 nm (63,425 mol^{-1} dm^3 cm^{-1}). Emission (CHCl$_3$) λ$_{em}$ 391 nm. Anal. Calcd for $C_{34}H_{28}Cl_8N_4O_4$: C, 48.60; H, 3.36; N, 6.67; O, 7.62; found: C, 48.40; H, 3.60; N, 6.72; O, 7.98.

4.1.2.5. (1α,2β,5α,6β,21β,22α,25β,26α)-8,19,28,38-Tetraaza-1,6,21,26-tetrachloro-1,41,42,42-tetramethoxyundecacyclo [24.14.1.1.^{6,21}.0^{2,25}.0^{5,22}.0^{7,20}.0^{9,18}.0^{11,16}.0^{27,40}.0^{29,38}.0^{31,36}]dote-tracontane-7(20), 8,10,12,14,16,18,27(40),28,30,32,34,36-tetra-deca-ene (D1f). Reaction time 10 h, yield 90%. Mp>300 °C; IR (KBr) 3056 (w), 2981 (m), 2947 (m), 2843 (m), 1551 (m), 1456 (m), 1189 cm^{-1} (s); ^{1}H NMR (400 MHz, CDCl$_3$) δ 8.79 (s, 4H), 8.14 (dd, J=6.4, 3.5 Hz, 4H), 7.64 (dd, J=6.4, 3.5 Hz, 4H), 3.61 (s, 6H), 3.37 (s, 6H), 2.72 (d, J=10.2 Hz, 4H), 2.15 (d, J=11.6 Hz, 4H), 0.19 (dd, J=10.2, 9.6 Hz, 4H); ^{13}C NMR (100 MHz, CDCl$_3$) δ 153.3 (s), 138.7 (s), 133.4 (s), 128.3 (d), 127.8 (d), 127.0 (d), 109.2 (s), 75.8 (s), 52.2 (q), 51.8 (q), 49.3 (d), 22.1 (t); MS (FAB) 807 (3) [M+H+6]$^+$, 805 (8) [M+H+4]$^+$, 803 (7) [M+H+2]$^+$, 154 (100); UV/vis (CHCl$_3$) λ$_{abs}$ (ε) 279, 350, 367 nm (151,873 mol^{-1} dm^3 cm^{-1}). Emission (CHCl$_3$) λ$_{em}$ 479 nm. Anal. Calcd for $C_{42}H_{36}Cl_4N_4O_4$: C, 62.85; H, 4.52; N, 6.98; O, 7.97; found: C, 62.81; H, 4.72; N, 7.14; O, 7.81.

4.1.2.6. (1α,2β,3α,4β,15β,16α,19β,20α)-6,13,22,29-Tetraaza-1,4,15,20-tetrachloro-31,31,32,32-tetramethoxynoncyclo [18.10.1.1.^{14,15}.0^{2,19}.0^{3,16}.0^{5,14}.0^{7,12}.0^{21,30}.0^{23,28}]dotriacontane-5 (14),6,8,10,12,17,21(30),22,24,26,28-undecaene (D2a). Reaction time 15 min, yield 92%. Mp>300 °C; IR (KBr) 3060 (w), 2974 (m), 2942 (m), 2924 (m), 2902 (m), 2839 (m), 1511 (m), 1462 (m), 1199 cm^{-1} (s); ^{1}H NMR (400 MHz, CDCl$_3$) δ 8.25 (m, 2H), 8.16 (m, 2H), 7.79 (m, 4H), 5.20 (d, J=1.0 Hz, 2H), 3.80 (s, 6H), 3.40 (d, J=10.1 Hz, 2H), 3.39 (s, 6H), 2.43 (d, J=10.1 Hz, 2H); ^{13}C NMR (100 MHz, CDCl$_3$) δ 152.3 (s), 151.6 (s), 142.5 (s), 142.2 (s), 130.0 (d), 129.8 (d), 129.3 (d), 129.3 (d), 110.5 (s), 75.6 (s), 74.7 (s), 52.3 (q), 52.1 (q), 43.3 (d), 38.1 (d); MS (FAB) 676 (3) [M+6]$^+$, 674 (7) [M+4]$^+$, 672 (6) [M+2]$^+$, 670 (2) [M]$^+$, 154 (100); UV/vis (CHCl$_3$) λ$_{abs}$ (ε) 245, 321, 332 nm (70,453 mol^{-1} dm^3 cm^{-1}). Emission (CHCl$_3$) λ$_{em}$ 390 nm. HRMS (FAB) calcd for $C_{32}H_{27}Cl_4N_4O_4$ [M+H]$^+$: 671.0786; found: 671.0789.

4.1.2.7. (1α,2β,3α,4β,15β,16α,19β,20α)-6,13,22,29-Tetraaza-1,4,15,20-tetrachloro-31,31,32,32- tetramethoxy-9,10,25,26-tetrame-thylnoncyclo[18.10.1.1.^{14,15}.0^{2,19}.0^{3,16}.0^{5,14}.0^{7,12}.0^{21,30}.0^{23,28}]-do-triacontane-5(14),6,8,10,12,17,21(30),22,24,26,28-undecaene (D2b). Reaction time 15 min, yield 94%. Mp>300 °C; IR (KBr) 2983 (w), 2949 (s), 2839 (m), 1499 (s), 1194 cm^{-1} (s); ^{1}H NMR (400 MHz, CDCl$_3$): δ 8.01 (s, 2H), 7.91 (s, 2H), 5.17 (d, J=1.0 Hz, 2H), 3.79 (s, 6H), 3.38 (s, 6H), 3.37 (d, J=10.1 Hz, 2H), 2.51 (s, 6H), 2.48 (s, 6H), 2.41 (dd, J=10.1, 1.1 Hz, 2H); ^{13}C NMR (100 MHz, CDCl$_3$): δ 151.3 (s), 150.7 (s), 141.4 (s), 141.0 (s), 140.5 (s), 140.3 (s), 128.7 (d), 128.6 (d), 124.2 (d), 110.7 (s), 75.7 (s), 74.9 (s), 52.3 (q), 52.1 (q), 43.5 (d), 38.2 (d), 20.3 (q); MS (FAB) 732 (6) [M+6]$^+$, 730 (15) [M+4]$^+$, 728 (14) [M+2]$^+$, 726 (3) [M]$^+$, 154 (100); UV/vis (CHCl$_3$) λ$_{abs}$ (ε) 254, 329, 344 nm (73,839 mol^{-1} dm^3 cm^{-1}). Emission (CHCl$_3$) λ$_{em}$ 380 nm. HRMS (FAB) calcd for $C_{36}H_{35}Cl_4N_4O_4$ [M+H]$^+$: 727.1412; found:

727.1419. Anal. Calcd for $C_{36}H_{34}Cl_4N_4O_4$: C, 59.35; H, 4.70; N, 7.69; O, 8.78; found: C, 59.19; H, 4.77; N, 7.67; O, 8.76.

4.1.2.8. (1α,2β,3α,4β,15β,16α,19β,20α)-6,13,22,29-Tetraaza-1,4,15,20-tetrachloro-9,10,25,26,31, 31,32,32-octamethoxynonacyclo [18.10.1.1.^{14,15}.0^{2,19}.0^{3,16}.0^{5,14}.0^{7,12}.0^{21,30}.0^{23,28}]dotriacontane-5 (14),6,8,10,12,17,21(30),22,24,26,28-undecaene (D2c). Reaction time 15 min, yield 94%. Mp>300 °C; IR (KBr) 2995 (m), 2948 (s), 2844 (m), 1631 (m), 1504 (s), 1469 (s), 1429 (s), 1243 cm^{-1} (s); ^{1}H NMR (400 MHz, CDCl$_3$) δ 7.55 (s, 2H), 7.46 (s, 2H), 5.19 (s, 2H), 4.07 (s, 6H), 4.01 (s, 6H), 3.78 (s, 6H), 3.37 (s, 6H), 3.36 (d, J=10.1 Hz, 2H), 2.42 (d, J=10.1 Hz, 2H); ^{13}C NMR (100 MHz, CDCl$_3$) δ 152.5 (s), 152.4 (s), 149.8 (s), 149.0 (s), 139.5 (d), 139.2 (d), 124.3 (d), 111.1 (s), 107.6 (s), 107.5 (s), 75.9 (s), 75.0 (s), 56.4 (q), 56.4 (q), 52.3 (q), 52.1 (q), 43.8 (d), 38.4 (d); MS (FAB) 796 (2) [M+6]$^+$, 790 (2) [M]$^+$, 154 (100); UV/vis (CHCl$_3$) λ$_{abs}$ (ε) 250, 361 nm (43,856 mol^{-1} dm^3 cm^{-1}). Emission (CHCl$_3$) λ$_{em}$ 381 nm. HRMS (FAB) calcd for $C_{36}H_{35}Cl_4N_4O_8$ [M+H]$^+$: 791.1209; found: 791.1215. Anal. Calcd for $C_{36}H_{34}Cl_4N_4O_8$ (794.51): C, 54.56; H, 4.32; N, 7.07; O, 16.15; found: C, 54.28; H, 4.34; N, 7.14; O, 16.32.

4.1.2.9. (1α,2β,3α,4β,15β,16α,19β,20α)-6,13,22,29-Tetraaza-1,4,9,10,15,20,25,26-hexachloro-31, 31,32,32-tetramethoxynoncyclo [18.10.1.1.^{14,15}.0^{2,19}.0^{3,16}.0^{5,14}.0^{7,12}.0^{21,30}.0^{23,28}]dotriacontane-5 (14),6,8,10,12,17, 21(30),22,24,26,28-undecaene (D2d). Reaction time 15 min, yield 93%. Mp>300 °C; IR (KBr) 3082 (w), 2982 (m), 2950 (s), 2845 (m), 1474 (s), 1194 cm^{-1} (s); ^{1}H NMR (400 MHz, CDCl$_3$) δ 8.37 (s, 2H), 8.27 (s, 2H), 5.19 (d, J=1.1 Hz, 2H), 3.80 (s, 6H), 3.37 (s, 6H), 3.35 (d, J=10.1 Hz, 2H), 2.44 (dd, J=10.1, 1.1 Hz, 2H); ^{13}C NMR (100 MHz, CDCl$_3$) δ 153.6 (s), 152.9 (s), 141.2 (s), 141.0 (s), 134.8 (s), 134.7 (s), 130.1 (d, 2C), 124.3 (d), 110.5 (s), 75.5 (s), 74.6 (s), 52.5 (q), 52.3 (q), 43.3 (d), 38.1 (d); MS (FAB) 813 (4) [M+8]$^+$, 811 (5) [M+6]$^+$, 809 (4) [M+4]$^+$, 807 (3) [M+2]$^+$, 154 (100); UV/vis (CHCl$_3$) λ$_{abs}$ (ε) 249, 344 nm (67,546 mol^{-1} dm^3 cm^{-1}). Emission (CHCl$_3$) λ$_{em}$ 391 nm. HRMS (FAB) calcd for $C_{32}H_{23}Cl_8N_4O_4$ [M+H]$^+$: 806.9228; found: 806.9229. Anal. Calcd for $C_{32}H_{22}Cl_8N_4O_4$: C, 47.44; H, 2.74; N, 6.92; O, 7.90; found: C, 47.48; H, 2.43; N, 7.05; O, 8.02.

4.1.2.10. (1α,2β,3α,4β,15β,16α,19β,20α)-6,13,22,29-Tetraaza-1,4,15,20-tetrachloro-31,31,32,32-tetramethoxy-9,10,25,26-tetrani-trononcyclo[18.10.1.1.^{14,15}.0^{2,19}.0^{3,16}.0^{5,14}.0^{7,12}.0^{21,30}.0^{23,28}]do-triacontane-5(14),6,8,10,12,17,21(30),22,24,26,28-undecaene (D2e). Reaction time 12 h, yield 89%. Mp>300 °C; IR (KBr) 3080 (m), 3000 (m), 2954 (m), 2898 (w), 2846 (m), 1541 (s), 1353 (s), 1197 cm^{-1} (s); ^{1}H NMR (400 MHz, CDCl$_3$) δ 8.84 (s, 2H), 8.73 (s, 2H), 5.25 (d, J=1.1 Hz, 2H), 3.84 (s, 6H), 3.41 (s, 6H), 3.41 (d, J=10.1 Hz, 2H), 2.53 (dd, J=10.1, 1.1 Hz, 2H); ^{13}C NMR (100 MHz, CDCl$_3$) δ 157.5 (s), 156.8 (s), 143.0 (s), 142.9 (s), 142.7 (s), 142.6 (s), 142.5 (d), 127.3 (d), 124.4 (d), 110.8 (s), 75.5 (s), 74.5 (s), 52.7 (q), 52.5 (q), 43.2 (d), 38.1 (d); MS (FAB) 858 (w) [M+8]$^+$, 856 (w) [M+6]$^+$, 854 (2) [M+4]$^+$, 852 (w) [M+2]$^+$, 850 (1) [M]$^+$, 154 (100); UV/vis (CHCl$_3$) λ$_{abs}$ (ε) 262 nm (58,220 mol^{-1} dm^3 cm^{-1}). HRMS (FAB) calcd for $C_{32}H_{23}Cl_4N_8O_{12}$ [M+H]$^+$: 851.0189; found: 851.0198. Anal. Calcd for $C_{32}H_{22}Cl_4N_8O_{12}$: C, 45.09; H, 2.60; N, 13.15; O, 22.52; found: C, 45.18; H, 2.79; N, 13.09; O, 22.62.

4.1.2.11. (1α,2β,3α,4β,19β,20α,23β,24α)-6,17,26,37-Tetraaza-1,4,19,24-tetrachloro-39,39,40,40-tetramethoxyundecacyclo [22.14.1.1.^{14,19}.0^{2,23}.0^{3,20}.0^{5,18}.0^{7,16}.0^{9,14}.0^{25,38}.0^{27,36}.0^{29,34}]tetra-contane-5(18),6,8,10,12,14,16,21,25(38),26,28,30,32,34,35-pentade-caene (D2f). Reaction time 15 min, yield 93%. Mp>300 °C; IR (KBr) 3055 (w), 2981 (m), 2947 (m), 2843 (m), 1551 (m), 1456 (m), 1189 cm^{-1} (s); ^{1}H NMR (400 MHz, CDCl$_3$) δ 8.83 (s, 2H), 8.72 (s, 2H), 8.15 (dd, J=7.8, 2.7 Hz, 2H), 8.10 (dd, J=7.8, 2.7 Hz, 2H), 7.63 (m, 4H), 5.24 (s, 2H), 3.85 (s, 6H), 3.50 (d, J=10.1 Hz, 2H), 3.43 (s, 6H), 2.52 (d, J=10.1 Hz, 2H); ^{13}C NMR (100 MHz, CDCl$_3$) δ 153.0 (s),

152.5 (s), 138.9 (s), 138.5 (s), 133.5 (s), 133.4 (s), 128.3 (d, 2C), 128.0 (d), 127.9 (d), 127.1 (d), 127.1 (d), 124.2 (d), 109.7 (s), 75.6 (s), 74.7 (s), 52.3 (q), 52.1 (q), 43.1 (d), 38.0 (d); MS (FAB) 776 (2) $[M+6]^+$, 774 (5) $[M+4]^+$, 772 (5) $[M+2]^+$, 770 (2) $[M]^+$, 136 (100); UV/vis (CHCl$_3$) λ_{abs} (ϵ) 280, 350, 368 nm (98,362 mol^{-1} dm^3 cm^{-1}). Emission (CHCl$_3$) λ_{em} 484 nm. HRMS (FAB) calcd for C$_{40}$H$_{31}$Cl$_4$N$_4$O$_4$ $[M+H]^+$: 771.1099; found: 771.1088. Anal. Calcd for C$_{40}$H$_{30}$Cl$_4$N$_4$O$_4$: C, 62.19; H, 3.91; N, 7.25; O, 8.28; found: C, 62.16; H, 4.14; N, 6.93; O, 8.43.

4.1.2.12. (1α,2β,3α,4β,15β,16α,23β,24α)-6,13,26,33-Tetraaza-1,4,15,24-tetrachloro-35,35,36,36-tetramethoxydecacyclo[22.10.1.1^{4,15}.0^{2,23}.0^{3,16}.0^{5,14}.0^{7,12}.0^{17,22}.0^{25,34}.0^{27,32}]hexatriacontane-5(14),6,8,10,12,17(22),18,20,25(34),26,28,30,21-tridecaene (D3a). Reaction time 15 min, yield 99%. Mp 287–289 °C; IR (KBr) 3059 (w), 2974 (m), 2942 (m), 2924 (m), 2902 (m), 2839 (m), 1511 (m), 1462 (m), 1199 cm^{-1} (s); ^{1}H NMR (400 MHz, CDCl$_3$) δ 8.20 (d, J=8.1 Hz, 2H), 7.71 (m, 4H), 7.61 (dd, J=8.1 Hz, 2H), 6.87 (dd, J=6.2, 3.4 Hz, 2H), 6.80 (dd, J=6.2, 3.4 Hz, 2H), 3.87 (s, 6H), 3.81 (d, J=10.7 Hz, 2H), 3.39 (s, 6H), 3.10 (d, J=10.7 Hz, 2H); ^{13}C NMR (100 MHz, CDCl$_3$) δ 151.8 (s), 151.6 (s), 142.2 (s), 142.1 (s), 129.7 (d), 129.6 (d), 129.1 (d), 128.8 (d), 128.5 (d), 126.8 (d), 110.2 (s), 77.6 (s), 75.5 (s), 52.3 (q), 46.1 (d), 39.2 (d); MS (FAB) 727 (5) $[M+7]^+$, 725 (21) $[M+5]^+$, 723 (39) $[M+3]^+$, 721 (29) $[M+1]^+$, 154 (100); UV/vis (CHCl$_3$) λ_{abs} (ϵ) 245, 320, 331 nm (60,404 mol^{-1} dm^3 cm^{-1}). Emission (CHCl$_3$) λ_{em} 390 nm. Anal. Calcd for C$_{36}$H$_{28}$Cl$_4$N$_4$O$_4$: C, 59.85; H, 3.91; N, 7.76; O, 8.86; found: C, 59.91; H, 3.74; N, 7.60; O, 9.13.

4.1.2.13. (1α,2β,3α,4β,15β,16α,23β,24α)-6,13,26,33-Tetraaza-1,4,15,24-tetrachloro-35,35,36,36-tetramethoxy-9,10,29,30-tetramethyldecacyclo[22.10.1.1^{4,15}.0^{2,23}.0^{3,16}.0^{5,14}.0^{7,12}.0^{17,22}.0^{25,34}.0^{27,32}]hexatricontane-5(14),6,8,10,12,17(22),18,20,25(34),26,28,30,32-tridecaene (D3b). Reaction time 15 min, yield 95%. Mp>300 °C; IR (KBr) 2949 (s), 2839 (m), 1499 (s), 1194 cm^{-1} (s); ^{1}H NMR (400 MHz, CDCl$_3$) δ 7.94 (s, 2H), 7.45 (s, 2H), 6.89 (dd, J=6.2, 3.4 Hz, 2H), 6.85 (dd, J=6.2, 3.4 Hz, 2H), 3.85 (s, 6H), 3.77 (d, J=10.7 Hz, 2H), 3.37 (s, 6H), 3.09 (d, J=10.7 Hz, 2H), 2.46 (s, 6H), 2.36 (s, 6H); ^{13}C NMR (100 MHz, CDCl$_3$) δ 150.8 (s), 150.5 (s), 141.1 (s), 140.9 (s), 140.1 (s), 139.9 (s), 128.7 (d), 128.3 (d), 128.1 (s), 127.1 (d), 126.9 (d), 110.3 (s), 77.8 (s), 75.6 (s), 52.3 (q), 52.3 (q), 46.1 (d), 39.2 (d), 20.3 (q), 20.2 (q); MS (FAB) 784 (7) $[M+8]^+$, 780 (24) $[M+4]^+$, 776 (9) $[M]^+$, 154 (100); UV/vis (CHCl$_3$) λ_{abs} (ϵ) 254, 329, 344 nm (61,442 mol^{-1} dm^3 cm^{-1}). Emission (CHCl$_3$) λ_{em} 380 nm. HRMS (FAB) calcd for C$_{40}$H$_{37}$Cl$_4$N$_4$O$_4$ $[M+H]^+$: 777.1563; found: 777.1566. Anal. Calcd for C$_{40}$H$_{36}$Cl$_4$N$_4$O$_4$ (778.55): C, 61.71; H, 4.66; N, 7.20; O, 8.22; found: C, 61.60; H, 4.65; N, 6.97; O, 8.17.

4.1.2.14. (1α,2β,3α,4β,15β,16α,23β,24α)-6,13,26,33-Tetraaza-1,4,15,24-tetrachloro-9,10,29,30,35,35,36,36-octamethoxydecacyclo[22.10.1.1^{4,15}.0^{2,23}.0^{3,16}.0^{5,14}.0^{7,12}.0^{17,22}.0^{25,34}.0^{27,32}]hexatriacontane-5(14),6,8,10,12,17(22),18,20,25(34),26,28,30,32-tridecaene (D3c). Reaction time 15 min, yield 91%. Mp>300 °C; IR (KBr) 2948 (s), 2844 (m), 1631 (m), 1504 (s), 1469 (s), 1429 (s), 1243 cm^{-1} (s); ^{1}H NMR (400 MHz, CDCl$_3$) δ 7.50 (s, 2H), 7.00 (s, 2H), 6.88 (m, 4H), 4.06 (s, 6H), 3.88 (s, 6H), 3.85 (s, 6H), 3.76 (d, J=10.7 Hz, 2H), 3.38 (s, 6H), 3.09 (d, J=10.7 Hz, 2H); ^{13}C NMR (100 MHz, CDCl$_3$) δ 152.2 (s), 152.1 (s), 149.3 (s), 148.9 (s), 139.2 (s), 139.0 (s), 128.9 (s), 127.0 (d), 126.9 (d), 110.7 (s), 107.2 (d), 107.0 (d), 77.8 (s), 75.7 (s), 56.4 (q), 56.3 (q), 52.3 (q), 52.2 (q), 46.5 (d), 39.3 (d); MS (FAB) 848 (w) $[M+8]^+$, 842 (1) $[M+2]^+$, 840 (1) $[M]^+$, 154 (100); UV/vis (CHCl$_3$) λ_{abs} (ϵ) 250, 361 nm (37,357 mol^{-1} dm^3 cm^{-1}). Emission (CHCl$_3$) λ_{em} 381 nm. HRMS (FAB) calcd for C$_{40}$H$_{37}$Cl$_4$N$_4$O$_8$ $[M+H]^+$: 841.1391; found: 841.1378. Anal. Calcd for C$_{40}$H$_{36}$Cl$_4$N$_4$O$_8$: C, 57.02; H, 4.31; N, 6.65; O, 15.19; found: C, 56.69; H, 4.13; N, 6.62; O, 15.27.

4.1.2.15. (1α,2β,3α,4β,15β,16α,23β,24α)-6,13,26,33-Tetraaza-1,4,9,10,15,24,29,30-octachloro-35,35,36,36-tetramethoxydecacyclo

[22.10.1.1^{4,15}.0^{2,23}.0^{3,16}.0^{5,14}.0^{7,12}.0^{17,22}.0^{25,34}.0^{27,32}]hexatriacontane-5(14),6,8,10,12,17(22),18,20,25(34),26,28,30,32-tridecaene (D3d). Reaction time 15 min, yield 98%. Mp>300 °C; IR (KBr) 3082 (w), 2982 (m), 2950 (s), 2845 (m), 1474 (s), 1194 cm^{-1} (s); ^{1}H NMR (400 MHz, CDCl$_3$) δ 8.32 (s, 2H), 7.82 (s, 2H), 6.94 (m, 2H), 6.89 (m, 2H), 3.86 (s, 6H), 3.76 (d, J=10.7 Hz, 2H), 3.38 (s, 6H), 3.11 (d, J=10.7 Hz, 2H); ^{13}C NMR (100 MHz, CDCl$_3$) δ 153.2 (s), 152.9 (s), 140.9 (s), 140.7 (s), 134.5 (s), 134.3 (s), 129.8 (d), 129.5 (d), 128.2 (s), 127.6 (d), 127.0 (d), 110.2 (s), 77.5 (s), 75.4 (s), 52.4 (q), 52.4 (q), 46.0 (d), 39.1 (d); MS (FAB) 863 (18) $[M+8]^+$, 861 (24) $[M+6]^+$, 859 (22) $[M+4]^+$, 857 (10) $[M+2]^+$, 154 (100); UV/vis (CHCl$_3$) λ_{abs} (ϵ) 249, 344 nm (67,483 mol^{-1} dm^3 cm^{-1}). Emission (CHCl$_3$) λ_{em} 391 nm. HRMS (FAB) calcd for C$_{36}$H$_{25}$Cl$_8$N$_4$O$_4$ $[M+H]^+$: 856.9384; found: 856.9382. Anal. Calcd for C$_{36}$H$_{24}$Cl$_8$N$_4$O$_4$: C, 50.26; H, 2.81; N, 6.51; O, 7.44; found: C, 50.41; H, 3.15; N, 6.41; O, 7.56.

4.1.2.16. (1α,2β,3α,4β,15β,16α,23β,24α)-6,13,26,33-Tetraaza-1,4,15,24-tetrachloro-35,35,36,36-tetramethoxy-9,10,29,30-tetranitrodecacyclo[22.10.1.1^{4,15}.0^{2,23}.0^{3,16}.0^{5,14}.0^{7,12}.0^{17,22}.0^{25,34}.0^{27,32}]hexatriacontane-5(14),6,8,10,12,17(22),18,20,25(34),26,28,30,32-tridecaene (D3e). Reaction time 12 h, yield 93%. Mp>300 °C; IR (KBr) 3080 (m), 2954 (m), 2846 (m), 1541 (s), 1353 (s), 1197 cm^{-1} (s); ^{1}H NMR (400 MHz, CDCl$_3$) δ 8.78 (s, 2H), 8.28 (s, 2H), 7.00 (m, 4H), 3.90 (s, 6H), 3.83 (d, J=10.7 Hz, 2H), 3.40 (s, 6H), 3.20 (d, J=10.7 Hz, 2H); ^{13}C NMR (100 MHz, CDCl$_3$) δ 157.1 (s), 156.9 (s), 142.8 (s), 142.5 (s), 142.4 (s), 142.3 (s), 128.4 (d), 127.6 (s), 127.3 (s), 127.0 (d), 126.6 (d), 110.4 (s), 77.4 (s), 75.3 (s), 52.7 (q), 52.7 (q), 45.7 (d), 39.1 (d); MS (FAB) 906 (1) $[M+6]^+$, 904 (1) $[M+4]^+$, 902 (2) $[M+2]^+$, 900 (1) $[M]^+$, 154 (100); UV/vis (CHCl$_3$) λ_{abs} (ϵ) 261 nm (34,834 mol^{-1} dm^3 cm^{-1}). HRMS (FAB) calcd for C$_{36}$H$_{25}$Cl$_4$N$_8$O$_{12}$ $[M+H]^+$: 901.0346; found: 901.0342. Anal. Calcd for C$_{36}$H$_{24}$Cl$_4$N$_8$O$_{12}$ (902.43): C, 47.91; H, 2.68; N, 12.42; O, 21.27; found: C, 47.96; H, 2.68; N, 12.46; O, 21.16.

4.1.2.17. (1α,2β,3α,4β,19β,20α,27β,28α)-6,17,30,41-Tetraaza-1,4,19,28-tetrachloro-43,43,44,44-tetramethoxydodecacyclo[26.14.1.1^{14,19}.0^{2,27}.0^{3,20}.0^{5,18}.0^{7,16}.0^{9,14}.0^{21,26}.0^{29,42}.0^{31,40}.0^{33,38}]tetratetracontane-5(18),6,8,10,12,14,16,21(26),22,24,29(42),30,32,34,36,38,40-heptadecaene (D3f). Reaction time 15 min, yield 95%. Mp>300 °C; IR (KBr) 3055 (w), 2981 (m), 2947 (m), 2843 (m), 1551 (m), 1456 (m), 1189 cm^{-1} (s); ^{1}H NMR (400 MHz, CDCl$_3$) δ 8.78 (s, 2H), 8.26 (s, 2H), 8.11 (d, J=8.1 Hz, 2H), 7.96 (d, J=8.1 Hz, 2H), 7.57 (m, 4H), 6.86 (dd, J=6.2, 3.4 Hz, 2H), 6.79 (dd, J=6.2, 3.4 Hz, 2H), 3.91 (s, 6H), 3.90 (d, J=10.7 Hz, 2H), 3.43 (s, 6H), 3.22 (d, J=10.7 Hz, 2H); ^{13}C NMR (100 MHz, CDCl$_3$) δ 152.4 (s), 152.2 (s), 138.3 (s), 138.3 (s) 133.1 (s), 133.0 (s), 128.2 (d), 128.1 (d), 128.1 (d), 127.4 (d), 127.2 (d), 127.1 (d), 126.7 (d), 126.7 (d), 126.6 (d), 109.1 (s), 77.4 (s), 75.3 (s), 52.1 (q), 52.1 (q), 45.7 (d), 38.8 (d); MS (FAB): 828 (2) $[M+8]^+$, 826 (8) $[M+6]^+$, 824 (16) $[M+4]^+$, 822 (16) $[M+2]^+$, 820 (5) $[M]^+$, 136 (100); UV/vis (CHCl$_3$) λ_{abs} (ϵ) 280, 351, 368 nm (153,621 mol^{-1} dm^3 cm^{-1}). Emission (CHCl$_3$) λ_{em} 484 nm. HRMS (FAB) calcd for C$_{44}$H$_{33}$Cl$_4$N$_4$O$_4$ $[M+H]^+$: 821.1256; found: 821.1258. Anal. Calcd for C$_{44}$H$_{32}$Cl$_4$N$_4$O$_4$: C, 64.25; H, 3.92; N, 6.81; O, 7.78; found: C, 64.64; H, 3.91; N, 6.77; O, 7.92.

4.1.2.18. (1α,2β,3α,4β,15β,16α,19β,20α)-6,8,13,22,27,29-Hexaaza-1,4,15,20-tetrachloro-31,31,32,32-tetramethoxynoncyclo[18.10.1.1^{4,15}.0^{2,19}.0^{3,16}.0^{5,14}.0^{7,12}.0^{21,30}.0^{23,28}]dotriacontane-5(14),6,8,10,12,17,21(30),22,24,26,28-undecaene (D2gα). Reaction time 8 h, yield 81%. Mp 280–281 °C; IR (KBr): 2952 (m), 2848 (w), 1738 (s), 1500 (s), 1195 (s); ^{1}H NMR (400 MHz, CDCl$_3$): δ 9.18 (dd, J=4.2, 1.9 Hz, 2H), 8.52 (dd, J=8.3, 1.9 Hz, 2H), 7.76 (dd, J=8.3, 4.2 Hz, 2H), 5.17 (d, J=1.1 Hz, 2H), 3.80 (s, 6H), 3.53 (d, J=10.1 Hz, 2H), 3.37 (s, 6H), 2.50 (dd, J=10.1, 1.1 Hz, 2H); ^{13}C NMR (100 MHz, CDCl$_3$): δ 155.4 (s), 154.1 (s), 153.0 (d), 151.5 (s), 138.4 (s), 137.7 (d), 125.3 (d), 124.5 (d), 110.8 (s), 75.5 (s), 74.8 (s), 52.4 (q), 52.3 (q), 43.4 (d), 38.1 (d); UV/vis (mixture, CDCl$_3$): λ_{abs} (ϵ) 310, 323 nm (46,318 mol^{-1} dm^3 cm^{-1}); MS

(FAB): 678 (25) $[M+6]^+$, 676 (62) $[M+4]^+$, 672 (7) $[M]^+$, 154 (100); HMRS (FAB) calcd for $C_{30}H_{25}Cl_4N_6O_4$ $[M+H]^+$: 673.0701, found: 673.0696. Anal. Calcd for $C_{30}H_{24}Cl_4N_6O_4$ (672.39): C, 53.43; H, 3.59; N, 12.46; O, 9.49; found: C, 53.25; H, 3.86; N, 12.26; O, 9.21.

4.1.2.19. (1α,2β,3α,4β,15β,16α,23β,24α)-6,8,13,26,31,33-Hexaaza-1,4,15,24-tetrachloro-35,35,36, 36-tetramethoxydecacyclo[22.10.1.1^{4,15}.0^{2,23}.0^{3,16}.0^{5,14}.0^{7,12}.0^{17,22}.0^{25,34}.0^{27,32}]hexatria-contane-5 (14),6,8,10,12,17(22),18,20,25(34),26,28,30,21-tridecaene (**D3gα**). - Reaction time 8 h, yield 76%. Mp 280–281 °C; IR (KBr): 2952 (m), 2848 (w), 1738 (s), 1500 (s), 1195 (s); ^{1}H NMR (400 MHz, CDCl$_3$): δ 9.10 (dd, J=4.2, 1.9 Hz, 2H), 8.08 (dd, J=8.3, 1.9 Hz, 2H), 7.60 (dd, J=8.3, 4.2 Hz, 2H), 6.86 (dd, J=6.2, 3.4 Hz, 2H), 6.84 (dd, J=6.2, 3.4 Hz, 2H), 3.93 (d, J=10.7 Hz, 2H), 3.87 (s, 6H), 3.39 (s, 6H), 3.23 (d, J=10.7 Hz, 2H); ^{13}C NMR (100 MHz, CDCl$_3$): δ 155.4 (s), 153.7 (s), 152.7 (d), 150.9 (s), 138.1 (s), 137.6 (d), 128.7 (s), 127.4 (d), 126.9 (d), 125.1 (d), 110.4 (s), 77.6 (s), 75.3 (s), 52.5 (q), 52.4 (q), 45.8 (d), 39.1 (d); UV/vis (mixture, CHCl$_3$): λ_{abs} (ϵ) 311, 325 nm (47,406 mol^{-1} dm^3 cm^{-1}); MS (FAB) 730 (17) $[M+8]^+$, 728 (32) $[M+6]^+$, 726 (73) $[M+4]^+$, 725 (100) $[M+H+2]^+$, 724 (47) $[M+2]^+$, 722 (11) $[M]^+$; HMRS (FAB) calcd for $C_{34}H_{27}Cl_4N_6O_4$ $[M+H]^+$: 723.0848, found: 723.0852. Anal. Calcd for $C_{34}H_{26}Cl_4N_6O_4$ (724.42): C, 56.37; H, 3.62; N, 11.60; O, 8.83; found: C, 56.38; H, 3.85; N, 11.84; O, 8.64.

Table 3
Crystal data and structure refinement for compounds **D1a**, **D2a**, **D2f**, **D3f**, **D2g-α**, and **D3g-α**

Identification code	D1a	D2a	D2f
Empirical formula	$C_{34}H_{32}Cl_4N_4O_4-CH_2Cl_2$	$C_{32}H_{32}Cl_4N_4O_4$	$C_{40}H_{30}Cl_4N_4O_4-2CHCl_3$
Formula weight	787.36	672.37	1011.22
Crystal size [mm]	0.1×0.1×0.1	0.1×0.2×0.2	0.1×0.2×0.2
Temperature [K]	273(2)	273(2)	273(2)
Wavelength [Å]	0.71073	0.71073	0.71073
Crystal system, Space group	Monoclinic, $P2(1)/c$	Orthorhombic, $Pca2(1)$	Monoclinic, $C2/c$
Unit cell dimensions	a=11.8176(5) Å	a=19.142(8) Å	a=23.6348(19) Å
	b=12.8470(6) Å	b=8.024(3) Å	b=8.1528(6) Å
	c=23.9534(11) Å	c=19.142(8) Å	c=23.8433(19) Å
	α=90°	α=90°	α=90°
	β=102.6280(10)°	β=90°	β=107.666(2)°
	γ=90°	γ=90°	γ=90°
Volume [Å^3]	3548.7(3)	2940(2)	4377.7(6)
Z	4	4	4
Density (calcd) [mg/m^3]	1.474	1.519	1.534
Absorption coefficient [mm^{-1}]	0.530	0.450	0.685
F(000)	1624	1384	2056
θ range for data collection [°]	1.74–28.29	2.13–28.38	1.79–28.33
Index ranges	−15≤h≤15, −16≤k≤16, −31≤l≤31	−24≤h≤25, −10≤k≤10, −25≤l≤25	−31≤h≤30, −10≤k≤10, −31≤l≤31
Reflections collected	31,111	24,551	24,551
Independent reflections	8579[R_{int}=0.0276]	6986[R_{int}=0.1018]	5315[R_{int}=0.0543]
Completeness to θ=28.29	97.2%	97.2%	97.4%
Refinement method	Full-matrix least-squares on $F2$	Full-matrix least-squares on $F2$	Full-matrix least-squares on $F2$
Data/restraints/parameters	8579/0/447	6986/1/401	6986/1/401
Goodness-of-fit on F^2	1.076	1.054	1.652
Final R indices [$I>2(I)$]	R1=0.0380, wR2=0.1124	R1=0.0448, wR2=0.1050	R1=0.1397, wR2=0.4183
R indices (all data)	R1=0.0440, wR2=0.1155	R1=0.0481, wR2=0.1064	R1=0.1651, wR2=0.4384
$\triangle\rho_{max}$, $\triangle\rho_{min}$ [e Å^{-3}]	0.386, −0.340	0.375 and −0.498	2.911 and −1.301

Identification code	D3f	D2g-α	D3g-α
Empirical formula	$C_{44}H_{32}Cl_4N_4O_4-2CHCl_3$	$C_{30}H_{24}Cl_4N_6O_4$	$C_{34}H_{26}Cl_4N_6O_4-CHCl_3$
Formula weight	1061.27	674.35	843.78
Crystal size [mm]	0.1×0.2×0.2	0.1×0.2×0.2	0.1×0.2×0.2
Temperature [K]	273(2)	273(2)	273(2)
Wavelength [Å]	0.71073	0.71073	0.71073
Crystal system, Space group	Triclinic, $P-1$	Monoclinic, $P2(1)/n$	Monoclinic, $P2(1)/c$
Unit cell dimensions	a=12.0776(5) Å	a=13.5230(10) Å	a=20.4398(11) Å
	b=14.6795(7) Å	b=15.6055(12) Å	b=10.9182(6) Å
	c=15.1588(7) Å	c=15.0180(12) Å	c=17.6546(9) Å
	α=71.2790(10)°	α=90°	α=90°
	β=78.3720(10)°	β=113.2470(10)°	β=112.2060(10)°
	γ=67.2760(10)°	γ=90°	γ=90°
Volume [Å^3]	2338.51(18)	2912.0(4)	3647.7(3)
Z	2	4	4
Density (calcd) [mg/m^3]	1.507	1.538	1.536
Absorption coefficient [mm^{-1}]	0.645	0.456	0.594
F(000)	1080	1384	1720
θ range for data collection [°]	1.56–28.28	1.72–28.30	1.08–28.34
Index ranges	−16≤h≤15, −19≤k≤18, −19≤l≤20	−16≤h≤17, −20≤k≤20, −19≤l≤19	−27≤h≤27, −14≤k≤14, −23≤l≤23
Reflections collected	20,973	25,592	31,713
Independent reflections	10,833 [R_{int}=0.0286]	7057[R_{int}=0.0456]	8795[R_{int}=0.0633]
Completeness to θ=28.29	93.4%	97.6%	96.5%
Refinement method	Full-matrix least-squares on F^2	Full-matrix least-squares on F^2	Full-matrix least-squares on F^2
Data/restraints/parameters	10,833/0/582	7057/0/402	8795/0/474
Goodness-of-fit on F^2	1.194	1.078	1.023
Final R indices [$I>2(I)$]	R1=0.1001, wR2=0.2678	R1=0.0405, wR2=0.1212	R1=0.0746, wR2=0.2179
R indices (all data)	R1=0.1050, wR2=0.2720	R1=0.0446, wR2=0.1245	R1=0.1274, wR2=0.2455
$\triangle\rho_{max}$, $\triangle\rho_{min}$ [e Å^{-3}]	0.933 and −1.274	0.939 and −0.325	0.930 and −0.600

$R=\Sigma||F_o|-|F_c||/\Sigma|F_o|$.
$wR2=[\Sigma w(F_o^2-F_c^2)^2/\Sigma[w(F_o^2)^2]^{1/2}$.

4.2. X-ray crystallography

The X-ray crystallographic data were recorded with a Bruker AXS SMART APEX CCD X-ray diffractometer. Graphite monochromatized Mo Kα radiation [$\lambda=0.71073$ Å] and temperature of 298 (2) K were used. The CCD data were processed with SAINT and the structures were solved by direct method (SHELXS-97) and refined on F^2 by full-matrix least-squares techniques (SHELXL-97). Crystal data/structure refinement are compiled in Table 3.

Acknowledgements

Supplementary data

The experimental section (general) and proton NMR spectra of the Z-shaped quadruple-bridged [6,6] and [6,4]orthocyclophanes. Supplementary data associated with this article can be found in the online version, at doi:10.1016/j.tet.2010.10.065.

References and notes

1. (a) Meyer, E. A.; Castellano, R. K.; Diederich, F. *Angew. Chem., Int. Ed.* **2003**, *42*, 1210–1250; (b) Desiraju, G. R. *Acc. Chem. Res.* **2002**, *35*, 565–573; (c) Desiraju, G. R. *Acc. Chem. Res.* **1996**, *29*, 441–449; (d) Taylor, B.; Kennard, O. *Acc. Chem. Res.* **1984**, *17*, 320–326.
2. (a) Jennings, W. B.; Farrell, B. M.; Malone, J. F. *Acc. Chem. Res.* **2001**, *34*, 885–894; (b) Dunitz, J. D.; Gavezzotti, A. *Acc. Chem. Res.* **1999**, *32*, 677–684; (c) Ma, J. C.; Dougherty, D. A. *Chem. Rev.* **1997**, *97*, 1303–1324; (d) Jorgensen, W. L.; Severance, D. L. *J. Am. Chem. Soc.* **1990**, *112*, 4768–4774; (e) Hunter, C. A.; Sanders, J. K. M. *J. Am. Chem. Soc.* **1990**, *112*, 5525–5534; (f) Nishio, M.; Umezawa, Y.; Hirota, M.; Takeuchi, Y. *Tetrahedron* **1995**, *51*, 8665–8701; (g) Nishio, M.; Hirota, M. *Tetrahedron* **1989**, *45*, 7201–7245; (h) Cram, D. J.; Cram, J. M. *Acc. Chem. Res.* **1971**, *4*, 204–213.
3. (a) Boussicault, F.; Robert, M. *Chem. Rev.* **2008**, *108*, 2622–2645; (b) Burley, S. K.; Petsko, G. A. *Adv. Protein Chem.* **1988**, *39*, 125–189; (c) Burley, S. K.; Petsko, G. A. *Science* **1985**, *229*, 23–28; (d) Fokkens, M.; Jasper, C.; Schrader, T.; Koziol, F.; Ochsenfeld, C.; Polkowska, J.; Lobert, M.; Kahlert, B.; Klärner, F.-G. *Chem.—Eur. J.* **2005**, *11*, 477–494; (e) Kim, E.-i.; Paliwal, S.; Wilcox, C. S. *J. Am. Chem. Soc.* **1998**, *120*, 11192–11193; (f) Adrian, J. C., Jr.; Wilcox, C. S. *J. Am. Chem. Soc.* **1989**, *111*, 8055–8059.
4. (a) Harmata, M. *Acc. Chem. Res.* **2004**, *37*, 862–873; (b) Kläner, F.-G.; Kahlert, B. *Acc. Chem. Res.* **2003**, *36*, 919–932; (c) Fyfe, M. C. T.; Stoddart, J. F. *Acc. Chem. Res.* **1997**, *30*, 393–401; (d) Hunter, C. A. *Chem. Soc. Rev.* **1994**, 101–109; (e) Cram, D. J.; Bauer, R. H. *J. Am. Chem. Soc.* **1959**, *81*, 5971–5977.
5. (a) Chen, Y.; She, N.; Meng, X.; Yin, G.; Wu, A.; Isaacs, L. *Org. Lett.* **2007**, *9*, 1899–1902; (b) Kawase, T.; Kurata, H. *Chem. Rev.* **2006**, *106*, 5250–5273; (c) Wang, Z.-G.; Zhou, B.-H.; Chen, Y.-F.; Yin, G.-D.; Li, Y.-T.; Wu, A.-X.; Isaacs, L. *J. Org. Chem.* **2006**, *71*, 4502–4508; (d) Rebek, J., Jr. *Acc. Chem. Res.* **1999**, *32*, 278–286.
6. (a) Shibahara, M.; Watanabe, M.; Suenaga, M.; Ideta, K.; Matsumoto, T.; Shinmyozu, T. *Tetrahedron Lett.* **2009**, *50*, 1340–1344; (b) Muranaka, A.; Shibahara, M.; Watanabe, M.; Matsumoto, T.; Shinmyozu, T.; Kobayashi, N. *J. Org. Chem.* **2008**, *73*, 9125–9128; (c) Wong, W. W. H.; Diederich, F. *Chem.—Eur. J.* **2006**, *12*, 3463–3471; (d) Klärner, F.-G.; Burket, U.; Kamieth, M.; Boese, R. *J. Phys. Org.*

Chem. **2000**, *13*, 604–611; (e) Rowan, A. E.; Elemans, J. A. A. W.; Nolte, R. J. M. *Acc. Chem. Res.* **1999**, *32*, 995–1006; (f) Mataka, S.; Shigaki, K.; Sawada, T.; Mitoma, Y.; Taniguchi, M.; Thiemann, T.; Ohga, K.; Egashira, N. *Angew. Chem., Int. Ed.* **1998**, *37*, 2532–2534; (g) Mataka, S.; Mitoma, Y.; Thiemann, T.; Sawada, T.; Taniguchi, M.; Kobuchi, M.; Tashiro, M. *Tetrahedron* **1997**, *53*, 3015–3026.
7. (a) Head, N. J.; Oliver, A. M.; Look, K.; Lokan, N. R.; Jones, G. A.; Paddon-Row, M. N. *Angew. Chem., Int. Ed.* **1999**, *38*, 3219–3222; (b) Paddon-Row, M. N. *Acc. Chem. Res.* **1994**, *27*, 18–25.
8. (a) She, N.; Gao, M.; Cao, L.; Wu, A.; Isaacs, L. *Org. Lett.* **2009**, *11*, 2603–2606; (b) Stancl, M.; Necas, M.; Taraba, J.; Sindelar, V. *J. Org. Chem.* **2008**, *73*, 4671–4675; (c) Branchi, B.; Balzani, V.; Ceroni, P.; Kuchenbrandt, M. C.; Klärner, F.-G.; Bläser, D.; Boese, R. *J. Org. Chem.* **2008**, *73*, 5839–5851; (d) Reek, J. N. H.; Elemans, J. A. A. W.; de Gelder, R.; Beurskens, P. T.; Rowan, A. E.; Nolte, R. J. M. *Tetrahedron* **2003**, *59*, 175–185.
9. (a) Klärner, F.-G.; Kahlert, B.; Boese, R.; Bläser, D.; Juris, A.; Marchioni, F. *Chem. Eur. J.* **2005**, *11*, 3363–3374; (b) Klärner, F.-G.; Burkert, U.; Kamieth, M.; Boese, R.; Benet-Buchholz, J. *Chem.—Eur. J.* **1999**, *5*, 1700–1707; (c) Kurebayashi, H.; Sakaguchi, M.; Okajima, T.; Haino, T.; Usui, S.; Fukazawa, Y. *Tetrahedron Lett.* **1999**, *40*, 5545–5548.
10. (a) Chou, T.-C.; Liao, K.-C.; Lin, J.-J. *Org. Lett.* **2005**, *7*, 4843–4846; (b) Chou, T.-C.; Lin, K.-C.; Wu, C.-A. *Tetrahedron* **2009**, *65*, 10243–10257.
11. (a) Khan, F. A.; Prabhudas, B.; Dash, J. *J. Prakt. Chem.* **2000**, *342*, 512–517; (b) Ungnade, H. E.; McBee, E. T. *Chem. Rev.* **1958**, *58*, 249–320.
12. (a) Khan, F. A.; Dash, J.; Sudheer, C.; Sahu, N.; Parasuraman, K. *J. Org. Chem.* **2005**, *70*, 7565–7577; (b) Khan, F. A.; Dash, J. *J. Am. Chem. Soc.* **2002**, *124*, 2424–2425; (c) Khan, F. A.; Prabhudas, B.; Dash, J.; Sahu, N. *J. Am. Chem. Soc.* **2000**, *122*, 9558–9559.
13. (a) Garcia, J. G.; Fronczek, F. R.; McLaughlin, M. L. *Tetrahedron Lett.* **1991**, *32*, 3289–3292.
14. (a) Shibata, K.; Kulkarni, A. A.; Ho, D. M.; Pascal, R. A., Jr. *J. Am. Chem. Soc.* **1994**, *116*, 5983–5984; (b) Danish, A. A.; Silverman, M.; Tajima, Y. A. *J. Am. Chem. Soc.* **1954**, *76*, 6144–6150.
15. Chou, T.-C.; Hong, P.-C.; Lin, C.-T. *Tetrahedron Lett.* **1991**, *32*, 6351–6354.
16. Chou, T.-C.; Chiou, J.-H. *J. Chin. Chem. Soc.* **1986**, *33*, 227–234.
17. (a) Mataka, S.; Mimura, T.; Lee, S. T.; Kobayashi, H.; Takahashi, K.; Tashiro, M. *J. Org. Chem.* **1989**, *54*, 5237–5241; (b) Mataka, S.; Takahashi, K.; Mimura, T.; Hirota, T.; Takuma, K.; Kobayashi, H.; Tashiro, M.; Imada, K.; Kuniyoshi, M. *J. Org. Chem.* **1987**, *52*, 2653–2656.
18. Crystallographic data (excluding structure factors) for **D1a**, **D2a**, **D2f**, **D3f**, **D2g-α**, and **D3g-α** have been deposited with the Cambridge Crystallographic Data Centre as supplementary publication numbers CCDC 787937, CCDC 787936, CCDC 787935, CCDC 787933, CCDC 787934, and CCDC787932, respectively.
19. (a) Dorofeeva, O. V.; Mastryukov, V. S.; Allinger, N. L.; Almenningen, A. *J. Phys. Chem.* **1985**, *89*, 252–257; (b) Hendrickson, J. B. *J. Am. Chem. Soc.* **1967**, *89*, 7036–7043.
20. Chiang, J. F.; Bauer, S. H. *J. Am. Chem. Soc.* **1969**, *91*, 1898–1901.
21. Hydrogen bond is referred to the noncovalent interactions having interatomic distance shorter than the sum of the van der Waals radii of hydrogen (1.20 Å) and carbon (1.70 Å), nitrogen (1.55 Å), oxygen (1.52 Å), or chlorine (1.75 Å) atoms.[22] Arbitrarily, we refer others having interatomic distance longer by about 25% as close contacts.
22. (a) Pauling, L. *The Nature of the Chemical Bonds*; Cornel University: Ithaca, New York, NY, 1960; p 260; (b) Bondi, A. *J. Phys. Chem.* **1964**, *68*, 441–451.
23. (a) Paliwal, S.; Geib, S.; Wilcox, C. S. *J. Am. Chem. Soc.* **1994**, *116*, 4497–4498; (b) Kobayashi, K.; Asakawa, Y.; Kikuchi, Y.; Toi, H.; Aoyama, Y. *J. Am. Chem. Soc.* **1993**, *115*, 2648–2654; (c) Adams, H.; Carver, F. J.; Hunter, C. A.; Morales, J. C.; Seward, E. M. *Angew. Chem., Int. Ed. Engl.* **1996**, *35*, 1542–1544.
24. Taylor, B.; Kennard, O. *J. Am. Chem. Soc.* **1982**, *104*, 5063–5070.
25. (a) Gung, B. W.; Xue, X.; Reich, H. J. *J. Org. Chem.* **2005**, *70*, 3641–3644; (b) Sindkhedkar, M. D.; Mulla, H. R.; Cammers-Goodwin, A. *J. Am. Chem. Soc.* **2000**, *122*, 9271–9277.
26. (a) Carroll, W. R.; Pellechia, P.; Shimizu, K. D. *Org. Lett.* **2008**, *10*, 3547–3550; (b) Alkorta, I.; Blanco, F.; Elguero, J. *Tetrahedron Lett.* **2008**, *49*, 7246–7249.